

# Is the $\Lambda_c(2625)^+$ the heavy quark spin symmetry partner of the $\Lambda_c(2595)^+$ ?

Meng-Lin Du<sup>1,2,\*</sup>, Eliecer Hernández<sup>3,†</sup> and Juan Nieves<sup>1,‡</sup>

<sup>1</sup>*Instituto de Física Corpuscular (centro mixto CSIC-UV), Institutos de Investigación de Paterna, Apartado 22085, 46071, Valencia, Spain*

<sup>2</sup>*School of Physics, University of Electronic Science and Technology of China, Chengdu 611731, China*

<sup>3</sup>*Departamento de Física Fundamental e IUFFyM, Universidad de Salamanca, Plaza de la Merced s/n, E-37008 Salamanca, Spain*

 (Received 7 July 2022; accepted 22 November 2022; published 21 December 2022)

We use a  $\mathcal{O}(\alpha_s, \Lambda_{\text{QCD}}/m_c)$  heavy quark effective theory scheme, where only  $\mathcal{O}(\Lambda_{\text{QCD}}/m_b)$  corrections are neglected, to study the matrix elements of the scalar, pseudoscalar, vector, axial-vector and tensor currents between the  $\Lambda_b$  ground state and the odd parity charm  $\Lambda_c(2595)^+$  and  $\Lambda_c(2625)^+$  resonances. We show that in the near-zero recoil regime, the scheme describes reasonably well, taking into account uncertainties, the results for the 24 form factors obtained in lattice QCD (LQCD) just in terms of only four Isgur-Wise (IW) functions. We also find some support for the possibility that the  $\Lambda_c(2595)^+$  and  $\Lambda_c(2625)^+$  resonances might form a heavy quark spin symmetry (HQSS) doublet. However, we argue that the available LQCD description of these two resonances is not accurate enough to disentangle the possible effects of the  $\Sigma_c\pi$  and  $\Sigma_c^*\pi$  thresholds, located only a few MeV above their position, and that it cannot be ruled out that these states are not HQSS partners. Finally, we study the ratio  $\frac{d\Gamma[\Lambda_b \rightarrow \Lambda_{c,1/2}^* - \ell \bar{\nu}_\ell]/dq^2}{d\Gamma[\Lambda_b \rightarrow \Lambda_{c,3/2}^* - \ell \bar{\nu}_\ell]/dq^2}$  of the Standard Model differential semileptonic decay widths, with  $q$  the four-momentum transferred between the initial and final hadrons. We provide a natural explanation for the existence of large deviations, near the zero recoil, of this ratio from  $1/2$  (value predicted in the infinite heavy quark mass limit, assuming that the  $\Lambda_{c,1/2}^*$  and  $\Lambda_{c,3/2}^*$  are the two members of a HQSS doublet) based on S-wave contributions to the  $\Lambda_b \rightarrow \Lambda_{c,1/2}^*$  decay amplitude driven by a subleading IW function.

DOI: [10.1103/PhysRevD.106.114020](https://doi.org/10.1103/PhysRevD.106.114020)

## I. INTRODUCTION

Heavy quark symmetry plays an important role in our understanding of low-energy strong interactions and the classification of the heavy-light hadronic spectrum. In the infinite heavy quark mass limit ( $m_Q \rightarrow \infty$ ), the degrees of freedom of the infinitely massive heavy quark decouple from the light quark ones, and hence the heavy and light degrees of freedom are separately conserved. The dynamics of hadrons containing a heavy quark is blind to the flavor and spin of the heavy quark, with the latter exhibiting an  $\text{SU}(2)_Q$  pattern known as the heavy quark spin symmetry (HQSS). Light degrees of freedom (ldof) with spin-parity  $j_{\text{ldof}}^P$  yield to a degenerate doublet under rotations of the

heavy quark spin  $s_Q$ . The quantum numbers of this doublet are  $J^P = [j_{\text{ldof}} \pm \frac{1}{2}]^P$  since the spin-parity of the heavy quark is  $\frac{1}{2}^+$ . Note here that the ldof quantum numbers contain both the orbital angular-momentum and spin parts.

In the real world, HQSS is broken due to the large ( $m_Q \gg \Lambda_{\text{QCD}}$ ) but finite mass of the heavy quark, e.g.,  $c$  and  $b$  quarks. These doublets are not exactly degenerate with a hyperfine splitting of order  $\Lambda_{\text{QCD}}/m_Q$ . The similar masses of the isoscalar odd parity resonances  $\Lambda_c(2595)^+$  and  $\Lambda_c(2625)^+$ , with  $J^P = \frac{1}{2}^-$  and  $\frac{3}{2}^-$  respectively, makes them promising candidates for the lightest charmed baryon doublet with  $j_{\text{ldof}}^P = 1^-$ . This assignment has been widely adopted in the literature, see e.g., Refs. [1–7]. Various constituent quark models (CQMs) predict a nearly degenerate pair of P-wave charmed isoscalar baryons  $\Lambda_c^*$  with  $J^P = \frac{1}{2}^-$  and  $\frac{3}{2}^-$ , respectively, which masses are close to those of the  $\Lambda_c(2595)^+$  and  $\Lambda_c(2625)^+$  [3,8–10]. Two different orbital excitations are considered in Ref. [3], driven by the so-called  $\lambda$  and  $\rho$  degrees of freedom. While the former accounts for the excitation between the heavy quark and the light quark subsystem, the latter considers the excitation between the two light quarks. Owing to the big

\*du.ml@uestc.edu.cn

†gajatee@usal.es

‡jmnieves@ific.uv.es

*Published by the American Physical Society under the terms of the Creative Commons Attribution 4.0 International license. Further distribution of this work must maintain attribution to the author(s) and the published article's title, journal citation, and DOI. Funded by SCOAP<sup>3</sup>.*

difference between the heavy- and light-quark masses, the low-lying states are dominated by the lowest  $\lambda$ -mode excitation and the mixture with  $\rho$  excitations is small [3]. In this picture, the  $\Lambda_c(2595)^+$  and  $\Lambda_c(2625)^+$  correspond to the HQSS doublet associated to  $(\ell_\lambda = 1, \ell_\rho = 0)$  with total Idof spin  $s_{\text{Idof}} = 0$ , leading to  $j_{\text{Idof}}^P = 1^-$ . The predicted decay widths of these resonances within this scheme are found to be consistent with data [4,11].

The  $\Lambda_c(2595)^+$  and  $\Lambda_c(2625)^+$  have also been described in hadronic-molecular models, as the counterparts of the  $\Lambda(1405)$  and  $\Lambda(1520)$  with the strange quark replaced by the charm one [12–20]. Since the  $\Sigma_c$  and  $\Sigma_c^*$  form the ground  $j_{\text{Idof}}^P = 1^+$  HQSS doublet, the Idof quantum numbers of the S-wave  $\Sigma_c\pi$  and  $\Sigma_c^*\pi$  pairs are  $1^-$  for both cases. In Ref. [12], the  $\Lambda_c(2595)^+$  is dynamically generated from the S-wave scattering of the Goldstone bosons off the  $J^P = \frac{1}{2}^+$  charmed baryon octet. A similar treatment is performed in Ref. [19], where the masses of the  $\Lambda_c(2595)^+$  and  $\Lambda_c(2625)^+$  are reproduced as  $\Sigma_c\pi$  and  $\Sigma_c^*\pi$  bound states by fine-tuned parameters. A coupled-channel approach including the  $DN$  is studied in Ref. [13] for the  $\Lambda_c(2595)^+$ , and it is extended to the  $\Lambda_c(2625)^+$  sector subsequently in Refs. [14,15]. HQSS, however, is not respected since the  $D^*N$  channel is not considered and the  $D$  and  $D^*$  mesons form the ground  $j_{\text{Idof}}^P = 1/2^-$  HQSS doublet in the meson sector. The first molecular description of the  $\Lambda_c(2595)^+$  and  $\Lambda_c(2625)^+$  respecting HQSS was provided in Refs. [17,18], where the SU(3) Weinberg-Tomozawa chiral Lagrangian is extended to SU(6)<sub>lfs</sub>  $\times$  SU(2)<sub>Q</sub>, with lfs standing here for the spin-flavor symmetry in the light sector. The model is supplemented by a pattern of symmetry breaking corrections and using the particular renormalization scheme proposed in Refs. [14,16]. One  $J^P = \frac{3}{2}^-$  state is dynamically generated by the  $\Sigma_c^*\pi - D^*N$  coupled-channel dynamics, which is identified in [17] with the  $\Lambda_c(2625)^+$ , even though its mass is about 40 MeV larger and it is significantly wider than the physical resonance. Thus within this scheme, the  $\Lambda_c(2625)^+$  would be the counterpart of the  $\Lambda(1520)$  in the charm sector. Interestingly, the model of Refs. [17,18] produces two  $J^P = \frac{1}{2}^-$  states generated near the nominal position of the  $\Lambda_c(2595)^+$ . One is narrow and it strongly couples to  $DN$  and especially to  $D^*N$ , with a small mixing with  $\Sigma_c\pi$ . It is identified with the  $\Lambda_c(2595)^+$  resonance in Refs. [17,18]. The other  $J^P = \frac{1}{2}^-$  molecular state, however, is quite broad because of the sizable coupling to the open channel  $\Sigma_c\pi$ . The two states would be analogous to those forming the two-pole structure of the  $\Lambda(1405)$  [21–24], where the states couple to  $\Sigma\pi$  and  $\bar{K}N$ , respectively [24]. A big difference, between the charm and strange sectors, is that while  $D^*N$  plays a crucial role in the charm sector within the scheme of Refs. [17,18], the  $\bar{K}^*N$  channel is not considered in the chiral unitary approaches [21–24] because of the large  $\bar{K}^* - \bar{K}$  mass gap.

In Ref. [25], it is stressed that the narrow  $J^P = \frac{1}{2}^- \Lambda_c(2595)^+$  found in [17,18] is mostly generated from the  $DN - D^*N$  coupled-channel dynamics with a dominant  $j_{\text{Idof}}^P = 0^-$  configuration. The small coupling of this state to the  $\Sigma_c\pi$  channel is then a consequence of HQSS due to its small  $j_{\text{Idof}} = 1^-$  component. The coupling of the broad  $J^P = \frac{1}{2}^-$  state to the  $\Sigma_c\pi$ , however, is larger than those to  $DN$  and  $D^*N$  and thus dominated by the  $j_{\text{Idof}}^P = 1^-$  configuration. It means that the isoscalar  $J^P = \frac{3}{2}^- \Lambda_c(2625)^+$  state found in Refs. [17,18] would be the HQSS partner of the broad  $J^P = \frac{1}{2}^-$  state with  $j_{\text{Idof}}^P = 1^-$  [25], instead of the observed  $\Lambda_c(2595)^+$ . A similar two-pole structure for the  $J^P = \frac{1}{2}^-$  sector is found in Ref. [26] by making use of a SU(4) flavor extension of the local hidden gauge formalism. In that work, an additional broad state around 2675 MeV is found in the isoscalar  $J^P = \frac{3}{2}^-$  sector with the single-channel  $\Sigma_c^*\pi$  Weinberg-Tomozawa interaction, which would not be related to the  $\Lambda_c(2625)^+$ .

The interplay between the  $\Sigma_c^{(*)}\pi - D^{(*)}N$  baryon-meson pairs and the bare P-wave CQM states has been recently studied, in the framework of an effective field theory, respecting heavy quark spin and chiral symmetries [27]. It is shown that the  $\Lambda_c(2625)^+$  should be viewed mostly as a dressed three-quark state, which is originated from a bare CQM state. The  $\Lambda_c(2595)^+$ , however, should be either dynamically generated by the chiral  $\Sigma_c\pi$  interaction, or the result of the  $DN - D^*N$  coupled-channel dynamics with a  $j_{\text{Idof}}^P = 0^-$  configuration, depending on the employed renormalization procedure. In any case, these two resonances would not be HQSS partners [27]. This is because the bare  $J^P = \frac{3}{2}^-$  CQM state and the  $\Sigma_c\pi$  threshold are located extremely close to the  $\Lambda_c(2625)^+$  and  $\Lambda_c(2595)^+$ , respectively, and thus play different roles in each sector.

HQSS also puts constraints on the form factors of currents containing heavy quarks, based on the observation that the current  $\bar{Q}\Gamma q$  ( $\bar{Q}\Gamma Q'$ ) transforms as a spinor under SU(2)<sub>Q</sub> [SU(2)<sub>Q'</sub> as well] [28]. In particular in the heavy quark limit, the semileptonic decay of a  $\Lambda_b$  into the lowest HQSS doublet with  $j_{\text{Idof}}^P = 1^-$  can be described by a universal leading order Isgur-Wise (IW) function ( $\sigma$ ) [29]. Besides, at zero recoil, the weak-current matrix elements between a  $\Lambda_b$  and any excited charmed baryon vanish [1]. The form factors for the exclusive semileptonic  $\Lambda_b$  decays to the excited  $\Lambda_c$  baryons were first obtained to order  $\mathcal{O}(\Lambda_{\text{QCD}}/m_c)$  in heavy quark effective theory (HQET) in Ref. [30], and were improved to order  $\mathcal{O}(\Lambda_{\text{QCD}}/m_b)$  in Refs. [1,5], where the  $\Lambda_c(2595)^+$  and  $\Lambda_c(2625)^+$  were regarded as the lowest-lying  $j_{\text{Idof}}^P = 1^-$  doublet. At order  $\mathcal{O}(\Lambda_{\text{QCD}}/m_Q)$  (here  $Q = c$  and  $b$ ), there appear five additional independent functions ( $\sigma_1^{(c)}$ ,  $\phi_{\text{kin}}^{(c)}$ ,

$\phi_{\text{kin}}^{(b)}$ ,  $\phi_{\text{mag}}^{(c)}$  and  $\phi_{\text{mag}}^{(b)}$ ) and two low-energy constants (LECs)  $\bar{\Lambda}$  and  $\bar{\Lambda}'$ , following the notation introduced in Ref. [1]. The LECs ( $\bar{\Lambda}^{(l)}$ ) denote the energy in the hadron of the light degrees of freedom in the  $m_Q \rightarrow \infty$  limit. The functions  $\phi_{\text{kin}}^{(c)}$  and  $\phi_{\text{kin}}^{(b)}$  can be reabsorbed, neglecting  $\mathcal{O}(\Lambda_{\text{QCD}}^2/m_Q^2)$ , in the leading order IW function  $\sigma$ , common for both decays. Therefore, to describe the various form factors of the currents between the  $\Lambda_b$  and the  $\Lambda_{c,1/2}^*$  and  $\Lambda_{c,3/2}^*$  states at order  $\mathcal{O}(\Lambda_{\text{QCD}}/m_Q)$ , only three of these subleading functions and the two LECs  $\bar{\Lambda}$  and  $\bar{\Lambda}'$  are needed [25,30]. Furthermore, if the  $\mathcal{O}(\Lambda_{\text{QCD}}/m_b)$  corrections are neglected, and one only considers up to order  $\mathcal{O}(\Lambda_{\text{QCD}}/m_c)$ , all the form factors for the  $\Lambda_b \rightarrow \Lambda_{c,1/2}^*$ ,  $\Lambda_{c,3/2}^*$  transitions are given in terms of only three independent functions,  $\sigma(\omega)$ ,  $\phi_{\text{kin}}^{(c)}$  and  $\sigma_1^{(c)}$ , and the  $\bar{\Lambda}$  and  $\bar{\Lambda}'$  LECs [also see, for instance, Eqs. (31)–(33) of Ref. [25]]. The  $\Lambda_{\text{QCD}}/m_b$  or  $\Lambda_{\text{QCD}}^2/m_c^2$  contributions, not taken into account in this limit, are expected to be smaller than the theoretical uncertainties induced by the errors on  $(\bar{\Lambda} - \bar{\Lambda}')$ .

Moreover, the semileptonic form factors between the  $\Lambda_b$  and a final  $J^P = \frac{1}{2}^-$  charm baryon, but with  $j_{\text{ldof}}^P = 0^-$ , denoted as  $\Lambda_{c,1/2}^*$ , vanish in the  $m_Q \rightarrow \infty$  limit. The unique nonvanishing correction at order  $\mathcal{O}(\Lambda_{\text{QCD}}/m_c)$  comes from the chromomagnetic operator, which can be described by a universal function with a structure of the type  $\epsilon_{\mu\nu\rho\tau}\sigma^{\mu\nu}v^\rho v'^\tau$  with  $v$  and  $v'$  the four-velocities of the  $\Lambda_b$  and  $\Lambda_{c,1/2}^*$ , respectively [1]. Thus, the different HQSS pattern of form factors for the  $\Lambda_b$  semileptonic decay into a charm  $j_{\text{ldof}}^P = 1^-$  doublet or a  $j_{\text{ldof}}^P = 0^-$  singlet might be used to test whether the ldof configuration in the  $\Lambda_c(2595)^+$  corresponds mainly to any of these quantum numbers, provided that the decays are measured.

Given the lack of data for the form factors of the  $\Lambda_b \rightarrow \Lambda_c(2595)^+$  and  $\Lambda_b \rightarrow \Lambda_c(2625)^+$  semileptonic decays, the lattice QCD (LQCD) simulations carried out in Refs. [6,31] provide valuable information from first principles.<sup>1</sup> (In the second of the references, the exact zero-recoil rotational symmetry relations among the different form factors are imposed to ensure the correct behavior of the angular observables.) Using LQCD form factors [34–37], the line shape of the  $\Lambda_b \rightarrow \Lambda_c \mu^+ \bar{\nu}_\mu$  decay, with  $\Lambda_c$  the  $J^P = 1/2^+$  ground state charm baryon for which  $j_{\text{ldof}}^P = 0^+$ , has been found to be consistent with the LHCb measurement [38]. This gives strong support to the LQCD calculation of semileptonic form factors. Note, however, that the form factors for the  $\Lambda_b \rightarrow \Lambda_c$  and those

for the  $\Lambda_b \rightarrow \Lambda_{c,1/2}^*$ ,  $\Lambda_{c,3/2}^*$  transitions are not related at all, since the ldof in the final charm baryon have different configurations. In Ref. [1], branching fractions and heavy quark sum rules for  $\Lambda_b$  decays to  $\Lambda_c(2595)^+$  and  $\Lambda_c(2625)^+$  (identified as the HQSS doublet of  $j_{\text{ldof}}^P = 1^-$ ) within the Standard Model (SM) were evaluated in the large  $N_c$  limit of QCD, using the bound state soliton picture.

The relevant expressions for the matrix elements, up to order  $\alpha_s$  and  $\Lambda_{\text{QCD}}/m_Q$  in HQET, to test lepton flavor universality are provided in Ref. [5]. However in that work, only rough estimates of the form factors, obtained from the zero recoil sum rule [39,40], could be used. New physics signatures for various  $b \rightarrow c \ell \bar{\nu}_\ell$  four Fermi interactions in the baryon sector have been also investigated in Refs. [7,41], using a HQET-based parametrization of the form factors to existing quark model results [2] in the former, and the LQCD form factors obtained in [6,31] in the latter recent study, which is limited to a region close to zero recoil. As previously noted also in Ref. [6], the results of Ref. [7] show a tension between LQCD data and HQET predictions to order  $\alpha_s$  and  $\Lambda_{\text{QCD}}/m_Q$ , and points out to the existence of unexpectedly large HQET-violating terms, potentially large  $1/m_c^2$  corrections near zero recoil, in the LQCD form factors. Further studies of this issue are thus needed, since it is still an open question how well HQSS works for the semileptonic  $\Lambda_b \rightarrow \Lambda_c(2595)^+$  and  $\Lambda_b \rightarrow \Lambda_c(2625)^+$  transitions, and if the  $\Lambda_c(2595)^+$  and  $\Lambda_c(2625)^+$  form a HQSS doublet [27].

In this work, we will try to answer some of these questions using the LQCD form factors recently obtained in Refs. [6,31]. In Sec. II, we will provide the explicit definition of the  $\Lambda_b \rightarrow \Lambda_c^*$  semileptonic form factors used in this work, and the relations between them and those obtained in Refs. [6,31]. We briefly review the form factors in HQET, up to order  $\mathcal{O}(\alpha_s, \Lambda_{\text{QCD}}/m_c)$ , in Sec. III. We test how well HQSS describes these form factors and perform a detailed numerical analysis in Sec. IV. Section V includes a brief summary of the main results of this work. Finally in the Appendices A and B, we provide relations between the different sets of form factors considered in this work.

## II. FORM FACTORS FOR $\Lambda_b \rightarrow \Lambda_c^*$ SEMILEPTONIC TRANSITIONS

The form factors for the  $\Lambda_b \rightarrow \Lambda_c(2595)^+ \ell \bar{\nu}_\ell$  [ $\Lambda_b \rightarrow \Lambda_c(2625)^+ \ell \bar{\nu}_\ell$ ] semileptonic transitions parametrize the matrix elements of the local currents  $[\bar{c}(0)\Gamma b(0)]$  between the  $\Lambda_b$  and the  $\Lambda_c(2595)^+$  [ $\Lambda_c(2625)^+$ ] states. Following the notation of Ref. [1] for the vector and axial-vector currents and extending it to the scalar, pseudoscalar, and tensor currents, we have for the  $\Lambda_b \rightarrow \Lambda_c(2595)^+$

<sup>1</sup>The form factors for the  $\Lambda_b \rightarrow \Lambda_{c,1/2}^*$  and  $\Lambda_b \rightarrow \Lambda_{c,3/2}^*$  transitions have also been investigated within the framework of constituent quark models, see e.g., in Refs. [2,32,33].

$$\begin{aligned}
\langle \Lambda_c(2595)^+(p', s') | \bar{c}b | \Lambda_b(p, s) \rangle &= \tilde{d}_S \bar{u}_c(p', s') \gamma_5 u_b(p, s), \\
\langle \Lambda_c(2595)^+(p', s') | \bar{c} \gamma_5 b | \Lambda_b(p, s) \rangle &= \tilde{d}_P \bar{u}_c(p', s') u_b(p, s), \\
\langle \Lambda_c(2595)^+(p', s') | \bar{c} \gamma^\mu b | \Lambda_b(p, s) \rangle &= \bar{u}_c(p', s') \left[ \tilde{d}_{V_1} \gamma^\mu + \tilde{d}_{V_2} \frac{p^\mu}{m_{\Lambda_b}} + \tilde{d}_{V_3} \frac{p'^\mu}{m_{\Lambda_{c,1/2}^*}} \right] \gamma_5 u_b(p, s), \\
\langle \Lambda_c(2595)^+(p', s') | \bar{c} \gamma^\mu \gamma_5 b | \Lambda_b(p, s) \rangle &= \bar{u}_c(p', s') \left[ \tilde{d}_{A_1} \gamma^\mu + \tilde{d}_{A_2} \frac{p^\mu}{m_{\Lambda_b}} + \tilde{d}_{A_3} \frac{p'^\mu}{m_{\Lambda_{c,1/2}^*}} \right] u_b(p, s), \\
\langle \Lambda_c(2595)^+(p', s') | \bar{c} \sigma^{\mu\nu} \gamma_5 b | \Lambda_b(p, s) \rangle &= \bar{u}_c(p', s') \left[ i \frac{\tilde{d}_{T_1}}{m_{\Lambda_b}^2} (p^\mu p^\nu - p^\nu p^\mu) + i \frac{\tilde{d}_{T_2}}{m_{\Lambda_b}} (\gamma^\mu p^\nu - \gamma^\nu p^\mu) \right. \\
&\quad \left. + i \frac{\tilde{d}_{T_3}}{m_{\Lambda_b}} (\gamma^\mu p^\nu - \gamma^\nu p^\mu) + \tilde{d}_{T_4} \sigma^{\mu\nu} \right] u_b(p, s), \tag{1}
\end{aligned}$$

where  $m_{\Lambda_{c,1/2}^*}$  is the mass of  $\Lambda_c(2595)^+$ , and  $u_b(p, s)$  and  $u_c(p', s')$  are the spinors of  $\Lambda_b$  and  $\Lambda_c(2595)^+$  baryons, respectively ( $p$  and  $p'$  are four-momenta, while  $s$  and  $s'$  are spin indices). The form factors  $\tilde{d}_{S,P,V_i,A_i,T_i}$  are scalar functions of  $q^2 = (p - p')^2$ , or equivalently  $\omega = (m_{\Lambda_b}^2 + m_{\Lambda_{c,1/2}^*}^2 - q^2)/(2m_{\Lambda_b} m_{\Lambda_{c,1/2}^*})$ .

The form factor decomposition for the  $\langle \Lambda_c(2595)^+(p', s') | \bar{c} \sigma^{\mu\nu} b | \Lambda_b(p, s) \rangle$  matrix element can be straightforwardly obtained from that of the  $\sigma^{\mu\nu} \gamma_5$  operator by making use of  $\sigma^{\mu\nu} \gamma_5 = -\frac{i}{2} \epsilon^{\mu\nu\lambda\rho} \sigma_{\lambda\rho}$ , with the convention  $\epsilon_{0123} = +1$ .

Likewise, the  $\Lambda_b \rightarrow \Lambda_c(2625)^+$  matrix elements can be parametrized as

$$\begin{aligned}
\langle \Lambda_c(2625)^+(p', s') | \bar{c}b | \Lambda_b(p, s) \rangle &= \tilde{l}_S \frac{p^\lambda}{m_{\Lambda_b}} \bar{u}_{c,\lambda}(p', s') u_b(p, s), \\
\langle \Lambda_c(2625)^+(p', s') | \bar{c} \gamma_5 b | \Lambda_b(p, s) \rangle &= \tilde{l}_P \frac{p^\lambda}{m_{\Lambda_b}} \bar{u}_{c,\lambda}(p', s') \gamma_5 u_b(p, s), \\
\langle \Lambda_c(2625)^+(p', s') | \bar{c} \gamma^\mu b | \Lambda_b(p, s) \rangle &= \bar{u}_{c,\lambda}(p', s') \left[ \frac{p^\lambda}{m_{\Lambda_b}} \left( \tilde{l}_{V_1} \gamma^\mu + \tilde{l}_{V_2} \frac{p^\mu}{m_{\Lambda_b}} + \tilde{l}_{V_3} \frac{p'^\mu}{m_{\Lambda_{c,3/2}^*}} \right) + \tilde{l}_{V_4} g^{\lambda\mu} \right] u_b(p, s), \\
\langle \Lambda_c(2625)^+(p', s') | \bar{c} \gamma^\mu \gamma_5 b | \Lambda_b(p, s) \rangle &= \bar{u}_{c,\lambda}(p', s') \left[ \frac{p^\lambda}{m_{\Lambda_b}} \left( \tilde{l}_{A_1} \gamma^\mu + \tilde{l}_{A_2} \frac{p^\mu}{m_{\Lambda_b}} + \tilde{l}_{A_3} \frac{p'^\mu}{m_{\Lambda_{c,3/2}^*}} \right) + \tilde{l}_{A_4} g^{\lambda\mu} \right] \gamma_5 u_b(p, s), \\
\langle \Lambda_c(2625)^+(p', s') | \bar{c} \sigma^{\mu\nu} b | \Lambda_b(p, s) \rangle &= \bar{u}_{c,\lambda}(p', s') \left[ \frac{p^\lambda}{m_{\Lambda_b}} \left( i \frac{\tilde{l}_{T_1}}{m_{\Lambda_b}^2} (p^\mu p^\nu - p^\nu p^\mu) + i \frac{\tilde{l}_{T_2}}{m_{\Lambda_b}} (\gamma^\mu p^\nu - \gamma^\nu p^\mu) \right. \right. \\
&\quad \left. \left. + i \frac{\tilde{l}_{T_3}}{m_{\Lambda_b}} (\gamma^\mu p^\nu - \gamma^\nu p^\mu) + \tilde{l}_{T_4} \sigma^{\mu\nu} \right) + i \tilde{l}_{T_5} (g^{\lambda\mu} \gamma^\nu - g^{\lambda\nu} \gamma^\mu) + i \frac{\tilde{l}_{T_6}}{m_{\Lambda_b}} (g^{\lambda\mu} p^\nu - g^{\lambda\nu} p^\mu) \right] u_b(p, s), \tag{2}
\end{aligned}$$

where  $m_{\Lambda_{c,3/2}^*}$  is now the mass of  $\Lambda_c(2625)^+$ ,  $u_{c,\lambda}(p', s')$  is the Rarita-Schwinger spinor for the spin- $\frac{3}{2}$   $\Lambda_c(2625)^+$ , which satisfies  $p'^\lambda u_{c,\lambda} = \gamma^\lambda u_{c,\lambda} = 0$ , and the form factors  $\tilde{l}_{S,P,V_i,A_i,T_i}$  are scalar functions of  $q^2 = (p - p')^2$ , or  $\omega$ , which is now expressed in terms of  $m_{\Lambda_{c,3/2}^*}$ . Note there is also one more independent structure  $i \tilde{l}_{T_7} (g^{\lambda\mu} p^\nu - g^{\lambda\nu} p^\mu)/m_{\Lambda_b}$  in the form factor decomposition of the tensor operator, which cannot be eliminated simply by the equation of motion or transversality conditions. However, it is shown in Ref. [7] that the combination of operators,

$$\begin{aligned}
\mathcal{K}_{\mu\nu} &= \bar{u}_c^\lambda [v_\lambda (\sigma_{\mu\nu} - i(v'_\mu \gamma_\nu - v'_\nu \gamma_\mu)) + i(g_{\lambda\mu} [(\omega + 1) \gamma_\nu \\
&\quad - v_\nu - v'_\nu] - g_{\lambda\nu} [(\omega + 1) \gamma_\mu - v_\mu - v'_\mu])] u_b, \tag{3}
\end{aligned}$$

does not contribute to physical amplitudes. Here we have introduced the notations  $v_\mu = p_\mu/m_{\Lambda_b}$ ,  $v'_\mu = p'_\mu/m_{\Lambda_{c,3/2}^*}$  and  $\omega = v \cdot v'$ , determined by  $q^2$ . Thus, we can set to zero the contribution of  $\tilde{l}_{T_7}$  to the physical amplitudes by redefining  $\tilde{l}_{T_i}$  for  $i = 3, 4, 5, 6$ .

As in the case of the  $\Lambda_c(2595)^+$ , the  $\langle \Lambda_c(2625)^+(p', s') | \bar{c} \sigma^{\mu\nu} \gamma_5 b | \Lambda_b(p, s) \rangle$  form factors can be

obtained from the tensor ones introduced in the decomposition of the matrix element of the  $\sigma^{\mu\nu}$  operator.

The helicity form factors for  $\Lambda_b \rightarrow \Lambda_c(2595)^+$  and  $\Lambda_b \rightarrow \Lambda_c(2625)^+$  determined in the LQCD simulation carried out in Refs. [6,31] are linear combinations of those introduced above, and the relation between both sets of form factors is given in Appendix A.

### III. $\Lambda_b \rightarrow \Lambda_c^*$ FORM FACTORS AND HEAVY QUARK EFFECTIVE THEORY

In this section, we will provide the form factors for the semileptonic decay of the  $\Lambda_b$  into the members of the  $j_{\text{ldof}}^P = 1^-$  HQSS doublet  $\Lambda_{c,1/2}^*$  and  $\Lambda_{c,3/2}^*$  in HQET up to order  $\mathcal{O}(\Lambda_{\text{QCD}}/m_c)$  and including QCD short range logarithms [7,42].

In the infinite heavy quark limit ( $m_Q \rightarrow \infty$ ), the form factors  $\tilde{d}_i$  and  $\tilde{l}_i$  in Eqs. (1) and (2) for the  $\Lambda_b$  decay into the two members ( $\Lambda_c^*$ ) of the  $j_{\text{ldof}}^P = 1^-$  HQSS doublet can be described by a universal IW function [29]. In this limit, the ground state  $\Lambda_b$  is a HQSS singlet with  $j_{\text{ldof}}^P = 0^+$ , and thus can be described by a Dirac spinor  $u_b(v)$ , with  $v$  the velocity of the  $\Lambda_b$ , satisfying the condition  $\not{v}u_b(v) = u_b(v)$  [43]. For the  $j_{\text{ldof}}^P = 1^-$  doublet with velocity  $v'$ , the ldof are represented by a vector  $A^\mu$  subject to the transversality condition  $v' \cdot A = 0$ . Then, the  $\Lambda_c^*$  doublet can be introduced by the multiplet spinor,

$$\mathcal{U}_c^\mu(v') = A^\mu u_h(v'), \quad (4)$$

where the spinor  $u_h$  describes the heavy quark  $c$  obeying  $\not{v}'u_h = u_h$ . Note that  $\mathcal{U}_c^\mu(v')$  is not an irreducible representation under the Lorentz group, instead it contains both spin  $3/2 = (1 + 1/2)$  and  $1/2 = (1 - 1/2)$  components,

$$\mathcal{U}_c^\mu(v') = u_c^\mu(v') + \frac{1}{\sqrt{3}}(\gamma^\mu + v'^\mu)\gamma_5 u_c(v'), \quad (5)$$

where  $u_c^\mu(v')$  and  $u_c(v')$  are the Rarita-Schwinger and Dirac spinors for  $J^P = \frac{3}{2}^-$  and  $\frac{1}{2}^-$  states, respectively. Note that  $v' \cdot \mathcal{U}_c(v') = 0$ ,  $\not{v}'\mathcal{U}_c(v') = \mathcal{U}_c(v')$ , and  $\gamma_\mu u_c^\mu(v') = 0$ . Then one can easily obtain that in the  $m_Q \rightarrow \infty$  limit, the most general form for the matrix element respecting HQSS (i.e., being invariant under arbitrary separate rotations of the  $b$ - and  $c$ -quark spins [25]) is

$$\langle \Lambda_c^*; j_{\text{ldof}}^P = 1^- | \bar{h}_{v'}^{(c)} \Gamma h_v^{(b)} | \Lambda_b \rangle = \sigma(\omega) v_\lambda \bar{\mathcal{U}}_c^\lambda(v') \Gamma u_b(v), \quad (6)$$

where  $h_v^{(Q)}$  is the heavy quark field in HQET,  $\Gamma$  is a Dirac matrix, and  $\sigma(\omega)$  is the dimensionless leading IW function. Using Eqs. (5) and (6), one finds

$$\begin{aligned} \langle \Lambda_{c,1/2}^* | \bar{h}_{v'}^{(c)} \Gamma h_v^{(b)} | \Lambda_b \rangle &= \frac{1}{\sqrt{3}} \sigma(\omega) \bar{u}_c(\not{v}' - \omega) \gamma_5 \Gamma u_b, \\ \langle \Lambda_{c,3/2}^* | \bar{h}_{v'}^{(c)} \Gamma h_v^{(b)} | \Lambda_b \rangle &= \sigma(\omega) v_\lambda \bar{u}_c^\lambda \Gamma u_b, \end{aligned} \quad (7)$$

and thus, it is straightforward to obtain [25] the  $\tilde{d}_i$  and  $\tilde{l}_i$  form factors in terms of  $\sigma(\omega)$ .

At order  $\mathcal{O}(\Lambda_{\text{QCD}}/m_Q)$ , there are corrections originating from the matching of the  $b \rightarrow c$  flavor changing current onto the effective theory (HQET) and from order  $\mathcal{O}(\Lambda_{\text{QCD}}/m_Q)$  effective Lagrangian [1]. Considering for simplicity only  $\mathcal{O}(\Lambda_{\text{QCD}}/m_c)$  contributions, this is to say keeping invariance under rotations of the spin of the  $b$  quark, we have first for the current corrections [44]

$$\bar{c} \Gamma b = \bar{h}_{v'}^{(c)} \left( \Gamma - \frac{i}{2m_c} \not{D} \Gamma \right) h_v^{(b)}, \quad (8)$$

where  $D^\mu$  is the gauge covariant derivative. The charm quark next-leading order effective Lagrangian contains the kinetic energy and the chromomagnetic terms [44]

$$\delta \mathcal{L}_v^{(c)} = \frac{1}{2m_c} \bar{h}_{v'}^{(c)} \left( (iD_\perp)^2 + \frac{g_s}{2} \sigma \cdot G \right) h_{v'}^{(c)}. \quad (9)$$

The operator that appears in the correction of Eq. (8) can be parametrized as [30]

$$\begin{aligned} \bar{h}_{v'}^{(c)} i \not{D}_\lambda \Gamma h_v^{(b)} &= [\sigma_1^{(c)}(\omega) v_\mu v_\lambda + \sigma_2^{(c)}(\omega) v_\mu v'_\lambda \\ &+ \sigma_3^{(c)}(\omega) g_{\mu\lambda}] \bar{\Psi}_{v'}^{\mu(c)} \Gamma \Psi_v^{(b)}, \end{aligned} \quad (10)$$

with  $\Psi_{v'}^{\mu(c)}$  and  $\Psi_v^{(b)}$  the HQET fields which destroy the spin-1/2 and spin-3/2 members of the charm  $j_{\text{ldof}}^P = 1^-$  doublet and the ground state  $\Lambda_b$ , respectively. Multiplying Eq. (10) by  $v'^\lambda$  and making use of the equation of motion  $(v' \cdot D) h_{v'}^{(c)} = 0$ , one obtains  $\sigma_2^{(c)}(\omega) = -\omega \sigma_1^{(c)}(\omega)$ . Additionally, translational invariance allows to write [1]

$$\sigma_3^{(c)}(\omega) = (\bar{\Lambda} - \omega \bar{\Lambda}') \sigma(\omega) + (\omega^2 - 1) \sigma_1^{(c)}(\omega), \quad (11)$$

where, as already mentioned,  $\bar{\Lambda}(\bar{\Lambda}')$  denotes the energy, in the  $\Lambda_b(\Lambda_c^*)$  baryon, of the light degrees of freedom in the  $m_Q \rightarrow \infty$  limit. Then one has

$$\begin{aligned} \langle \Lambda_c^*; j_{\text{ldof}}^P = 1^- | \bar{h}_{v'}^{(c)} i \not{D} \Gamma h_v^{(b)} | \Lambda_b \rangle \\ = \bar{\mathcal{U}}_c^\mu(v') [v_\mu (\not{v}' - \omega) \sigma_1^{(c)}(\omega) + \gamma_\mu \sigma_3^{(c)}(\omega)] \Gamma u_b(v), \end{aligned} \quad (12)$$

and thus

$$\begin{aligned}
& \langle \Lambda_{c,1/2}^* | \bar{h}_{v'}^{(c)} i \not{D} \Gamma h_v^{(b)} | \Lambda_b \rangle \\
&= \frac{1}{\sqrt{3}} \bar{u}_c [(\omega^2 - 1) \sigma_1^{(c)}(\omega) - 3\sigma_3^{(c)}(\omega)] \gamma_5 \Gamma u_b, \\
& \langle \Lambda_{c,3/2}^* | \bar{h}_{v'}^{(c)} i \not{D} \Gamma h_v^{(b)} | \Lambda_b \rangle = \sigma_1^{(c)}(\omega) v_\lambda \bar{u}_c^\lambda (\not{\epsilon} - \omega) \Gamma u_b. \quad (13)
\end{aligned}$$

In addition, the correction  $\phi_{\text{kin}}^{(c)}(\omega)$  from the charm kinetic energy operator  $\bar{h}_{v'}^{(c)} (iD_\perp)^2 h_v^{(c)}$  in Eq. (9) respects HQSS and hence it enters in the same way as the leading IW function  $\sigma(\omega)$ , and it simply renormalizes the latter [1,30]:

$$\sigma(\omega) \rightarrow \tilde{\sigma}(\omega) = \sigma(\omega) + \frac{\phi_{\text{kin}}^{(c)}(\omega)}{2m_c}. \quad (14)$$

However, the chromomagnetic operator  $\bar{h}_{v'}^{(c)} g_s \sigma \cdot G h_v^{(c)} / 2$  breaks HQSS and it leads to a contribution to the matrix elements of  $\bar{h}_{v'}^{(c)} \Gamma h_v^{(b)}$  [1,30],

$$\begin{aligned}
& i\phi_{\text{mag}}^{(c)} g_{\mu\alpha} v_\nu \bar{u}_c^\alpha(v') \sigma^{\mu\nu} \frac{1 + \not{v}'}{2} \Gamma u_b(v) \\
&= \phi_{\text{mag}}^{(c)} v_\lambda \bar{u}_c^\lambda(v') \Gamma u_b(v) - \frac{2\phi_{\text{mag}}^{(c)}}{\sqrt{3}} \bar{u}_c(v') (\not{\epsilon} - \omega) \gamma_5 \Gamma u_b(v). \quad (15)
\end{aligned}$$

Combining the leading order [Eq. (7)], and the  $\mathcal{O}(\Lambda_{\text{QCD}}/m_c)$  [Eqs. (13)–(15)] contributions, we obtain that the general form of the semileptonic matrix elements, keeping the invariance under spin rotations of the quark  $b$ , reads [25]

$$\begin{aligned}
& \langle \Lambda_{c,1/2}^* | \bar{c} \Gamma b | \Lambda_b \rangle = \frac{1}{\sqrt{3}} \bar{u}_c [(\not{\epsilon} - \omega) \Delta_1(\omega) - \Delta_2(\omega)] \gamma_5 \Gamma u_b, \\
& \langle \Lambda_{c,3/2}^* | \bar{c} \Gamma b | \Lambda_b \rangle = v_\lambda \bar{u}_c^\lambda [\Omega_1(\omega) - (\not{\epsilon} - \omega) \Omega_2(\omega)] \Gamma u_b, \quad (16)
\end{aligned}$$

where we have introduced the scalar form factors

$$\begin{aligned}
\Delta_1(\omega) &= \sigma(\omega) + \frac{1}{2m_c} [\phi_{\text{kin}}^{(c)}(\omega) - 2\phi_{\text{mag}}^{(c)}(\omega)] \\
&= \tilde{\sigma}(\omega) - \frac{\phi_{\text{mag}}^{(c)}(\omega)}{m_c}, \\
\Delta_2(\omega) &= \frac{(\omega^2 - 1) \sigma_1^{(c)}(\omega) - 3\sigma_3^{(c)}(\omega)}{2m_c} \\
&= -\frac{2(\omega^2 - 1) \sigma_1^{(c)}(\omega) + 3(\bar{\Lambda} - \omega \bar{\Lambda}') \sigma(\omega)}{2m_c}, \\
\Omega_1(\omega) &= \sigma(\omega) + \frac{1}{2m_c} [\phi_{\text{kin}}^{(c)}(\omega) + \phi_{\text{mag}}^{(c)}(\omega)] \\
&= \tilde{\sigma}(\omega) + \frac{\phi_{\text{mag}}^{(c)}(\omega)}{2m_c}, \quad \Omega_2(\omega) = \frac{\sigma_1^{(c)}(\omega)}{2m_c}, \quad (17)
\end{aligned}$$

which are determined by the leading IW function  $\sigma$  and the subleading  $\mathcal{O}(\Lambda_{\text{QCD}}/m_c)$  correction discussed in Ref. [1].

The starting point in the construction of the low-energy effective theory is the observation that a very heavy quark bound inside a hadron moves more or less with the hadron's velocity  $v$ , and is almost on shell, i.e.,  $p_Q^\mu = m_Q v^\mu + k^\mu$ . Thus, HQET provides an expansion in powers of the residual momentum  $k$ , which is nominally  $\sim \Lambda_{\text{QCD}}$ , regardless of the momentum of the hadron [44]. Near zero recoil, one can set the four-velocities of the initial and final hadrons to be the same and one has a small residual momentum assigned to the outgoing hadron. However, the outgoing hadron momentum in the  $\Lambda_b$  rest frame soon becomes larger than  $\Lambda_{\text{QCD}}$ , reaching values around  $\sim 1.7(2.2)$  GeV in the end point of the spectrum for the tau (muon) semileptonic mode. Hence, far from zero recoil, the residual momentum will start to get large and then to keep  $k$  small, one should switch to a new effective theory with different four-velocities,  $v$  for the initial hadron and  $v'$  for the outgoing one, with  $\omega = v \cdot v'$  quickly deviating from one. Because of this mismatch of velocities, the leading IWs might rapidly decrease and the  $(\Delta_1, \Delta_2)$  or  $(\Omega_1, \Omega_2)$  hierarchy relations inferred from Eq. (17) far from zero recoil might not be as good as in the vicinity of  $\omega = 1$ . This observation does not dispute that the full QCD and HQET form factors must agree if one goes to high enough orders in the HQET expansion.

It is worth stressing that the  $\mathcal{O}(\Lambda_{\text{QCD}}/m_c)$  decomposition of Eq. (16) is valid for any  $\Lambda_b$  transition to  $J^P = \frac{1}{2}^-$  and  $J^P = \frac{3}{2}^-$  baryons, regardless of the ldof quantum numbers in the final charm states. This is so since Eq. (16) includes the most general breaking of the invariance under a spin rotation of the quark  $c$ . However, the expressions of the  $\Delta_{1,2}$  and  $\Omega_{1,2}$  form factors in terms of the leading and subleading IW functions given in Eq. (17) are specific to  $\Lambda_b$  decays into the two members of the  $j_{\text{ldof}}^P = 1^-$  HQSS doublet. Otherwise, the relations of Eq. (17) are lost and thus, for instance,  $\Delta_1(\omega)$  does not need to approach  $\Omega_1(\omega)$  in the heavy charm quark mass limit. This might be of special interest, since as we argued in the Introduction, the  $\Lambda_c(2595)^+$  [ $J^P = \frac{1}{2}^-$ ] could contain, in addition to  $j_{\text{ldof}}^P = 1^-$ , ldof components with  $j_{\text{ldof}}^P = 0^-$  quantum numbers. For the case of this latter unnatural transition, the matrix elements of the  $1/m_Q$  current and kinetic energy operator corrections are zero for the same reason that the leading form factor vanished [1]. The time ordered products involving the chromomagnetic operator lead to nonzero contributions, which however vanish at zero recoil [1] and can be cast in a  $\Delta_1$ -type form factor. To order  $1/m_Q$ , the corresponding  $\Delta_2$  form factor is therefore zero. These different HQSS patterns for the  $\Lambda_b$  semileptonic decay into a charm  $j_{\text{ldof}}^P = 1^-$  doublet or a  $j_{\text{ldof}}^P = 0^-$  singlet might shed light into the ldof configuration in the  $\Lambda_c(2595)^+$  resonance. Similarly, the  $J^P = \frac{3}{2}^-$   $\Lambda_c(2625)^+$

resonance could have, in addition to  $j_{\text{ldof}}^P = 1^-$ , a  $j_{\text{ldof}}^P = 2^-$  component. For this also unnatural  $0^+ \rightarrow 2^-$  transition, in contrast to what we saw for the  $j_{\text{ldof}}^P = 1^-$  component, the leading IW function and the kinetic energy operator correction vanish, as it occurs for the  $0^+ \rightarrow 0^-$  case [1,30]. Different to the latter case, the matrix element of the  $1/m_Q$  current term does not vanish for the

transition to  $j_{\text{ldof}}^P = 2^-$ , and it takes a form that can be absorbed into the  $\Omega_2(\omega)$  form factor. The chromomagnetic correction provides a  $1/m_c$ -suppressed contribution to  $\Omega_1(\omega)$ . Both corrections, however, vanish at zero recoil.

By employing Eq. (16), the  $\Lambda_{c,1/2}^*$  form factors up to  $\mathcal{O}(\alpha_s, \Lambda_{\text{QCD}}/m_c)$  order read

$$\begin{aligned}
\langle \Lambda_{c,1/2}^* | \bar{c}b | \Lambda_b \rangle &= -\frac{1}{\sqrt{3}} \bar{u}_c [(1 + \omega)(1 + C_S \hat{\alpha}_s) \Delta_1 + \Delta_2] \gamma_5 u_b, \\
\langle \Lambda_{c,1/2}^* | \bar{c} \gamma_5 b | \Lambda_b \rangle &= -\frac{1}{\sqrt{3}} \bar{u}_c [(\omega - 1)(1 + C_P \hat{\alpha}_s) \Delta_1 + \Delta_2] u_b, \\
\langle \Lambda_{c,1/2}^* | \bar{c} \gamma_\mu b | \Lambda_b \rangle &= \frac{1}{\sqrt{3}} \bar{u}_c \{ [(\omega - 1)(1 + C_{V_1} \hat{\alpha}_s) \Delta_1 + \Delta_2] \gamma_\mu - [2 + \hat{\alpha}_s(2C_{V_1} + C_{V_2}(\omega + 1))] \Delta_1 v_\mu \\
&\quad - C_{V_3} \hat{\alpha}_s(\omega + 1) \Delta_1 v'_\mu \} \gamma_5 u_b, \\
\langle \Lambda_{c,1/2}^* | \bar{c} \gamma_\mu \gamma_5 b | \Lambda_b \rangle &= \frac{1}{\sqrt{3}} \bar{u}_c \{ [(\omega + 1)(1 + C_{A_1} \hat{\alpha}_s) \Delta_1 + \Delta_2] \gamma_\mu - [2 + \hat{\alpha}_s(2C_{A_1} + C_{A_2}(\omega - 1))] \Delta_1 v_\mu \\
&\quad - C_{A_3} \hat{\alpha}_s(\omega - 1) \Delta_1 v'_\mu \} u_b, \\
\langle \Lambda_{c,1/2}^* | \bar{c} \sigma_{\mu\nu} \gamma_5 b | \Lambda_b \rangle &= -\frac{1}{\sqrt{3}} \bar{u}_c \{ i2C_{T_3} \hat{\alpha}_s \Delta_1 (v_\mu v'_\nu - v_\nu v'_\mu) + i[2 + \hat{\alpha}_s(2(C_{T_1} + C_{T_3}) + (\omega - 1)C_{T_2})] \Delta_1 (\gamma_\mu v_\nu - \gamma_\nu v_\mu) \\
&\quad - iC_{T_3} \hat{\alpha}_s(\omega + 1) \Delta_1 (\gamma_\mu v'_\nu - \gamma_\nu v'_\mu) + [(\omega - 1)(1 + \hat{\alpha}_s(C_{T_1} - C_{T_2} + C_{T_3})) \Delta_1 + \Delta_2] \sigma_{\mu\nu} \} u_b, \quad (18)
\end{aligned}$$

and for  $\Lambda_{c,3/2}^*$ ,

$$\begin{aligned}
\langle \Lambda_{c,3/2}^* | \bar{c}b | \Lambda_b \rangle &= \bar{u}_c^2 v_\lambda [(1 + C_S \hat{\alpha}_s) \Omega_1 + (\omega - 1) \Omega_2] u_b, \\
\langle \Lambda_{c,3/2}^* | \bar{c} \gamma_5 b | \Lambda_b \rangle &= \bar{u}_c^2 v_\lambda [(1 + C_P \hat{\alpha}_s) \Omega_1 + (\omega + 1) \Omega_2] u_b, \\
\langle \Lambda_{c,3/2}^* | \bar{c} \gamma_\mu b | \Lambda_b \rangle &= \bar{u}_c^2 v_\lambda \{ [(1 + C_{V_1} \hat{\alpha}_s) \Omega_1 + (\omega + 1) \Omega_2] \gamma_\mu + (C_{V_2} \hat{\alpha}_s \Omega_1 - 2\Omega_2) v_\mu + C_{V_3} \hat{\alpha}_s \Omega_1 v'_\mu \} u_b, \\
\langle \Lambda_{c,3/2}^* | \bar{c} \gamma_\mu \gamma_5 b | \Lambda_b \rangle &= \bar{u}_c^2 v_\lambda \{ [(1 + C_{A_1} \hat{\alpha}_s) \Omega_1 + (\omega - 1) \Omega_2] \gamma_\mu + (C_{A_2} \hat{\alpha}_s \Omega_1 - 2\Omega_2) v_\mu + C_{A_3} \hat{\alpha}_s \Omega_1 v'_\mu \} \gamma_5 u_b, \\
\langle \Lambda_{c,3/2}^* | \bar{c} \sigma_{\mu\nu} b | \Lambda_b \rangle &= \bar{u}_c^2 v_\lambda \{ i(2\Omega_2 - C_{T_2} \hat{\alpha}_s \Omega_1) (\gamma_\mu v_\nu - \gamma_\nu v_\mu) - iC_{T_3} \hat{\alpha}_s \Omega_1 (\gamma_\mu v'_\nu - \gamma_\nu v'_\mu) \\
&\quad + [(1 + C_{T_1} \hat{\alpha}_s) \Omega_1 + (\omega - 1) \Omega_2] \sigma_{\mu\nu} \} u_b, \quad (19)
\end{aligned}$$

where we have also included the  $\mathcal{O}(\hat{\alpha}_s = \alpha_s/\pi)$  perturbative corrections to the heavy quark currents, which are computed by matching QCD onto HQET [44]. We use the results of Eq. (9) and Appendix A of Ref. [42], where the known  $C_{\Gamma_i}(\omega)$  functions can also be found. The previous analysis of Ref. [7] also accounted for short range radiative effects. The approach adopted here differs from that used in this latter reference only by terms of the order of  $\mathcal{O}(\alpha_s \times \Lambda_{\text{QCD}}/m_c)$ . This is because in this work, for simplicity, we incorporate the  $\hat{\alpha}_s$  corrections also to the  $1/m_c$ -suppressed contributions induced by the subleading pieces of  $\Delta_1$  and  $\Omega_1$  IW functions. At the order we are working in the HQET expansion, these are higher-order terms and it is equally sounded to keep them finite or to set them to zero as in Ref. [7].

The matrix elements of Eqs. (18) and (19) can be used to express the form factors  $\tilde{d}_i$  and  $\tilde{l}_i$  in terms of  $\Delta_{1,2}$  and  $\Omega_{1,2}$ . The resulting scheme account up to order  $\mathcal{O}(\alpha_s, \Lambda_{\text{QCD}}/m_c)$  corrections. For the sake of clarity, we give the explicit expressions in Appendix B. We want to stress that, since the  $\mathcal{O}(\Lambda_{\text{QCD}}/m_c)$  decomposition of Eq. (16) is valid for any  $\Lambda_b$  transition to  $J^P = \frac{1}{2}^-$  and  $J^P = \frac{3}{2}^-$  baryons, regardless of the ldof quantum numbers in the final charm states, the form factors for  $\Lambda_b \rightarrow \Lambda_{c,1/2}^*, \Lambda_{c,3/2}^*$  in Eqs. (18) and (19) do not rely on the assumption that the final excited charm baryons form the lowest-lying  $J^P = 1^-$  HQSS ldof doublet, since  $\Delta_{1,2}$  and  $\Omega_{1,2}$  do not need to be related in principle. In other words, to order  $\mathcal{O}(\alpha_s, \Lambda_{\text{QCD}}/m_c)$ , Eqs. (18) and (19) give the most general form-factor decomposition for any

$\Lambda_b$  transition to  $J^P = \frac{1}{2}^-$  and  $J^P = \frac{3}{2}^-$  baryons independently of whether they belong to the same HQSS ldof doublet or not.

Neglecting radiative corrections, the  $\Lambda_b \rightarrow \Lambda_{c,1/2}^* \ell \bar{\nu}_\ell$  and  $\Lambda_b \rightarrow \Lambda_{c,3/2}^* \ell \bar{\nu}_\ell$  SM differential decay widths deduced from the vector and axial matrix elements in Eqs. (18) and (19) are given by [25]<sup>2</sup>

$$\begin{aligned} & \frac{d\Gamma[\Lambda_b \rightarrow \Lambda_{c,J^P}^*]}{d\omega} \\ &= (2J+1) \frac{8\Gamma_0}{3} \left(\frac{m_{\Lambda_c^*}}{m_{\Lambda_b}}\right)^3 \left(1 - \frac{m_\ell^2}{q^2}\right)^2 (\omega^2 - 1)^J \\ & \times \left\{ \alpha_J^2 \left[ 3\omega \frac{q^2 + m_\ell^2}{m_{\Lambda_b}^2} + 2 \frac{m_{\Lambda_c^*}}{m_{\Lambda_b}} (\omega^2 - 1) \left(1 + \frac{2m_\ell^2}{q^2}\right) \right] \right. \\ & + 2(\omega^2 - 1) [\alpha_1(\omega)\alpha_2(\omega)]_J \\ & \left. \times \left[ \frac{2q^2 + m_\ell^2}{m_{\Lambda_b}^2} + \left(1 - \frac{m_{\Lambda_c^*}^2}{m_{\Lambda_b}^2}\right) \left(1 + \frac{2m_\ell^2}{q^2}\right) \right] + \mathcal{O}\left(\alpha_s, \frac{\Lambda_{\text{QCD}}}{m_b}\right) \right\} \end{aligned} \quad (20)$$

with  $m_\ell$  the final charged lepton mass,  $\Gamma_0 = |V_{cb}|^2 G_F^2 m_{\Lambda_b}^5 / (192\pi^3)$ , where  $|V_{cb}|$  is the modulus of the Cabibbo-Kobayashi-Maskawa matrix element for the  $b \rightarrow c$  transition and  $G_F = 1.16638 \times 10^{-11} \text{ MeV}^{-2}$  is the Fermi decay constant, and

$$\begin{aligned} \alpha_{J=1/2}^2(\omega) &= \Delta_2^2(\omega) + (\omega^2 - 1)\Delta_1^2(\omega), \\ \alpha_1(\omega)\alpha_2(\omega)|_{J=1/2} &= \Delta_1(\omega)\Delta_2(\omega) \\ \alpha_{J=3/2}^2(\omega) &= \Omega_1^2(\omega) + (\omega^2 - 1)\Omega_2^2(\omega), \\ \alpha_1(\omega)\alpha_2(\omega)|_{J=3/2} &= \Omega_1(\omega)\Omega_2(\omega). \end{aligned} \quad (21)$$

In the strict  $m_c \rightarrow \infty$  limit,<sup>3</sup>

$$\lim_{m_c \rightarrow \infty} \left( \frac{d\Gamma[\Lambda_b \rightarrow \Lambda_{c,1/2}^*]/d\omega}{d\Gamma[\Lambda_b \rightarrow \Lambda_{c,3/2}^*]/d\omega} \right) = \frac{1}{2} \left( \frac{\lim_{m_c \rightarrow \infty} \Delta_1(\omega)}{\lim_{m_c \rightarrow \infty} \Omega_1(\omega)} \right)^2 \quad (22)$$

and if  $\Lambda_{c,1/2}^*$  and  $\Lambda_{c,3/2}^*$  are the two members of the  $J_{\text{ldof}}^P = 1^-$  HQSS doublet, the above ratio will be 1/2, since the

<sup>2</sup>We have numerically checked that the effects on the differential decay widths produced by the radiative corrections in Eqs. (18) and (19) are quite small. Actually, they are negligible when compared to the uncertainties induced on these distributions by the errors of the LQCD form factors. Therefore, for simplicity, we have not included the radiative corrections in the calculation of the differential decay widths, and to obtain Eq. (20), we have set all the  $C_{\Gamma_i}(\omega)$  functions to zero.

<sup>3</sup>Note that the  $(\omega^2 - 1)$  multiplying  $\Delta_1^2(\omega)$  compensates the overall extra  $(\omega^2 - 1)$  factor which appears for the  $J^P = 3/2^-$  decay width in Eq. (20).

relations of Eq. (17) will be satisfied and  $\Delta_1(\omega) \sim \Omega_1(\omega) \sim \sigma(\omega)$ . However in the vicinity of zero recoil ( $\omega \leq 1.05$ ), one might find large deviations, because in this kinematic region, the subleading contribution  $\Delta_2^2(\omega)$  to  $\alpha_{J=1/2}^2(\omega)$  could be comparable or larger than the other one,  $(\omega^2 - 1)\Delta_1^2(\omega)$ , which is used to obtain<sup>4</sup> Eq. (22). Actually, the  $\Delta_2(\omega)$  form factor accounts for an S-wave term to the  $\Lambda_b \rightarrow \Lambda_{c,1/2}^*$  decay amplitude proportional to  $3(\bar{\Lambda} - \bar{\Lambda}')\sigma(1)/(2m_c) \sim (0.2-0.3)\sigma(1)$  [25]. This follows from Eq. (17), using  $m_c \sim 1.4 \text{ GeV}$  for the charm quark mass,  $\bar{\Lambda} \sim 0.8 \text{ GeV}$  and  $\bar{\Lambda}' \sim 1 \pm 0.1 \text{ GeV}$  for the energies of the ldof, in the  $m_Q \rightarrow \infty$  limit, in the  $\Lambda_b$  and the P-wave  $\Lambda_{c,J^P}^*$  baryon. Since the SM  $\Lambda_b \rightarrow \Lambda_{c,3/2}^*$  semileptonic decay driven by the matrix elements in Eq. (19) occurs at least in P wave, it appears an extra factor  $(\omega^2 - 1)$ , and the ratio  $\frac{d\Gamma[\Lambda_b \rightarrow \Lambda_{c,1/2}^*]/d\omega}{d\Gamma[\Lambda_b \rightarrow \Lambda_{c,3/2}^*]/d\omega}$  could differ significantly from 1/2 when  $\omega$  is close to 1.

Notice that in the SM, there exist S-, P- and D-wave contributions to the  $1/2^+ \rightarrow 1/2^-$  semileptonic matrix element. D wave only involves the vector current, while both vector and axial currents appear in S and P waves. The S-wave terms are driven by the vector  $\tilde{d}_{V_1}$  and the combination  $(\tilde{d}_{A_1} + \tilde{d}_{A_2} + \tilde{d}_{A_3})$  of axial form factors, but the axial contribution vanishes in the massless lepton limit. From Appendix B, we see that both  $\tilde{d}_{V_1}$  and  $(\tilde{d}_{A_1} + \tilde{d}_{A_2} + \tilde{d}_{A_3})$  are proportional to  $\Delta_2(\omega = 1)$  at zero recoil, which gives rise to the S-wave  $\alpha_{J=1/2}^2$  term in the differential decay rate of Eq. (20). For the  $1/2^+ \rightarrow 3/2^-$  decay, the vector  $\tilde{l}_{V_4}$  accounts for the S-wave transition [1], while all the rest of the form factors account for higher-wave contributions. However, we see in Appendix B that this form factor is zero up to order  $\mathcal{O}(\alpha_s, \Lambda_{\text{QCD}}/m_c)$ , and hence the differential decay rate of Eq. (20) in this case proceeds at least in P wave. Actually, the leading contribution to  $\tilde{l}_{V_4}$  is of order  $\mathcal{O}(\Lambda_{\text{QCD}}/m_b)$  [1], but as we will show at the end of Sec. IV B, the consideration of this small contribution does not modify the theoretical expectation of finding large deviations from 1/2 for the ratio of differential decay rates close to zero recoil.

#### IV. NUMERICAL ANALYSIS

In the last two sections, we have presented a general parametrization and  $\mathcal{O}(\alpha_s, \Lambda_{\text{QCD}}/m_c)$  HQET form factors for the  $\Lambda_b \rightarrow \Lambda_{c,1/2}^*/\Lambda_{c,3/2}^*$  semileptonic transitions. Although in recent years the LHC has collected large numbers of  $\Lambda_b \rightarrow \Lambda_c(2595)^+ \mu^- \bar{\nu}_\mu$  and  $\Lambda_b \rightarrow \Lambda_c(2625)^+ \mu^- \bar{\nu}_\mu$  samples [38], the extraction of the form factors is, however, not available

<sup>4</sup>As can be seen in the right-bottom panel of Fig. 7, at  $\omega = 1.05$  one has that  $\Delta_2^2(\omega = 1.05) \approx 0.25\Delta_1^2(\omega = 1.05)$  which is 2.5 times larger than the corresponding value for  $(\omega^2 - 1)\Delta_1^2(\omega)$ .

yet. Without experimental input for the form factors, LQCD provides a valuable framework to test how well the  $J_{\text{ldof}}^P = 1^-$  HQSS predictions, with corrections of order  $\mathcal{O}(\alpha_s, \Lambda_{\text{QCD}}/m_c)$ , works to describe the  $\Lambda_c(2595)^+$  and  $\Lambda_c(2625)^+$  form factors measured on the lattice, and whether there is a possibility of a sizable  $J_{\text{ldof}}^P = 0^-$  configuration for the  $\Lambda_c(2595)^+$  resonance.

### A. LQCD and $\mathcal{O}(\Lambda_{\text{QCD}}/m_c)$ HQET form factors

The first LQCD calculation of the form factors for these transitions was carried out in Ref. [6], using three different ensembles of gauge-field configurations with  $2+1$  flavors of domain-wall fermions generated by the RBC and UKQCD collaborations [45,46], and three-quark interpolating fields to excite the  $\Lambda_c^*$  states. The form factors in Ref. [6] are defined through a helicity decomposition of the amplitudes and are evaluated at three unphysical pion masses,  $m_\pi=0.4312(13)$ ,  $0.3400(11)$  and  $0.3030(12)$  GeV. Finally, the results were extrapolated to the physical point (continuum limit and physical pion mass), where the LQCD form factors are parametrized as [6,31]

$$f(\omega) = F^f + A^f(\omega - 1), \quad (23)$$

which corresponds to a Taylor expansion around zero recoil  $\omega = 1$ . Because only two different close kinematics ( $\omega = 1.01$  and  $\omega = 1.03$ ) are available at the physical point in the LQCD calculation of Ref. [6], the

parametrization of Eq. (23) is expected to be only reliable for small  $(\omega - 1)$ . Systematic uncertainties are estimated from the variation of results obtained from two different extrapolations of the lattice results to the physical limit. The helicity form factors, which parametrize the matrix elements of the vector, axial-vector and tensor currents, for the two available values of  $\omega$  are treated in Ref. [6] as independent quantities. Thus, a total of 48 parameters were fitted to the lattice data. In the improved analysis carried out by the same authors in Ref. [31], relations among the different form factors at zero recoil, which follow from rotational symmetry, are imposed to ensure the correct behavior of the angular observables near the end point, and thus the number of free parameters is reduced to 39. In this work, we will employ the updated results of Ref. [31]. The form factors  $\tilde{d}_i$  and  $\tilde{l}_i$  introduced in Eqs. (1) and (2) are computed from the helicity form factors determined in Refs. [6,31] with the help of Eqs. (A1) and (A2), respectively.

As discussed in Sec. III, there are only two independent functions  $\Delta_{1,2}(\omega)$  and  $\Omega_{1,2}(\omega)$  for the  $\Lambda_b \rightarrow \Lambda_{c,1/2}^*$  and  $\Lambda_b \rightarrow \Lambda_{c,3/2}^*$  decays, respectively, including up to  $\mathcal{O}(\alpha_s, \Lambda_{\text{QCD}}/m_c)$  contributions; this is to say, neglecting  $\mathcal{O}(\Lambda_{\text{QCD}}/m_b)$  corrections. In order to test if the HQSS describes the semileptonic  $\Lambda_b \rightarrow \Lambda_c(2595)^+$  and  $\Lambda_b \rightarrow \Lambda_c(2625)^+$  decays at this order, we determine the  $\Delta_{1,2}(\omega)$  and  $\Omega_{1,2}(\omega)$  functions from two of the form factors in each of the transitions, and then predict the rest of the form factors using the relations collected in Appendix B. We take

$$\begin{aligned} \Delta_1(\omega) &= \frac{\sqrt{3}[\tilde{d}_{A_1}(\omega) - \tilde{d}_{V_1}(\omega)]}{2 + \hat{\alpha}_s[(1 + \omega)C_{A_1} + C_{V_1}(1 - \omega)]}, \\ \Delta_2(\omega) &= \frac{\sqrt{3}[(1 + \omega)(1 + C_{A_1}\hat{\alpha}_s)\tilde{d}_{V_1}(\omega) + (1 - \omega)(1 + C_{V_1}\hat{\alpha}_s)\tilde{d}_{A_1}(\omega)]}{2 + \hat{\alpha}_s[(1 + \omega)C_{A_1} + (1 - \omega)C_{V_1}]}, \\ \Omega_1(\omega) &= \frac{(1 - \omega)\tilde{l}_{V_1}(\omega) + (1 + \omega)\tilde{l}_{A_1}(\omega)}{2 + \hat{\alpha}_s[(1 - \omega)C_{V_1} + (1 + \omega)C_{A_1}]}, \\ \Omega_2(\omega) &= \frac{(1 + \hat{\alpha}_s C_{A_1})\tilde{l}_{V_1}(\omega) - (1 + \hat{\alpha}_s C_{V_1})\tilde{l}_{A_1}(\omega)}{2 + \hat{\alpha}_s[(1 - \omega)C_{V_1} + (1 + \omega)C_{A_1}]} \end{aligned} \quad (24)$$

As already mentioned,  $\hat{\alpha}_s = \alpha_s/\pi$  and the explicit expressions for the  $C_{\Gamma_i}$  can be found in Ref. [42]. Here there is a subtle point. We note that all types of contributions suppressed by any power of the charm quark mass should be included in the *unknown*  $\Delta_{1,2}$  and  $\Omega_{1,2}$  functions empirically determined from the LQCD form factors. Thus, we expect only  $\mathcal{O}(\Lambda_{\text{QCD}}/m_b)$  corrections, from the breaking of  $b$ -quark spin rotational invariance, to the matrix elements of the scalar, pseudoscalar, vector, axial-vector and tensor currents between the  $\Lambda_b$  ground state and the final odd parity charm  $\Lambda_c(2595)^+$  and  $\Lambda_c(2625)^+$

resonances, for the whole range of  $\omega$  values accessible in the decay.

The  $\Lambda_b \rightarrow \Lambda_c(2595)^+$  and  $\Lambda_b \rightarrow \Lambda_c(2625)^+$  form factors  $\tilde{d}_i$  and  $\tilde{l}_i$  evaluated using Eq. (B1) are compared with the LQCD results in Figs. 1 ( $1/2^+ \rightarrow 1/2^-$ ), 3 (vector and axial-vector  $1/2^+ \rightarrow 3/2^-$ ) and 5 (tensor  $1/2^+ \rightarrow 3/2^-$ ). There, the purple solid and blue dotted curves correspond to the LQCD results and the HQET predictions, obtained using the  $\Delta_{1,2}$  or  $\Omega_{1,2}$  functions determined as specified in Eq. (24), respectively. Statistic and systematic uncertainties, given in Refs. [6,31], are added in quadrature and

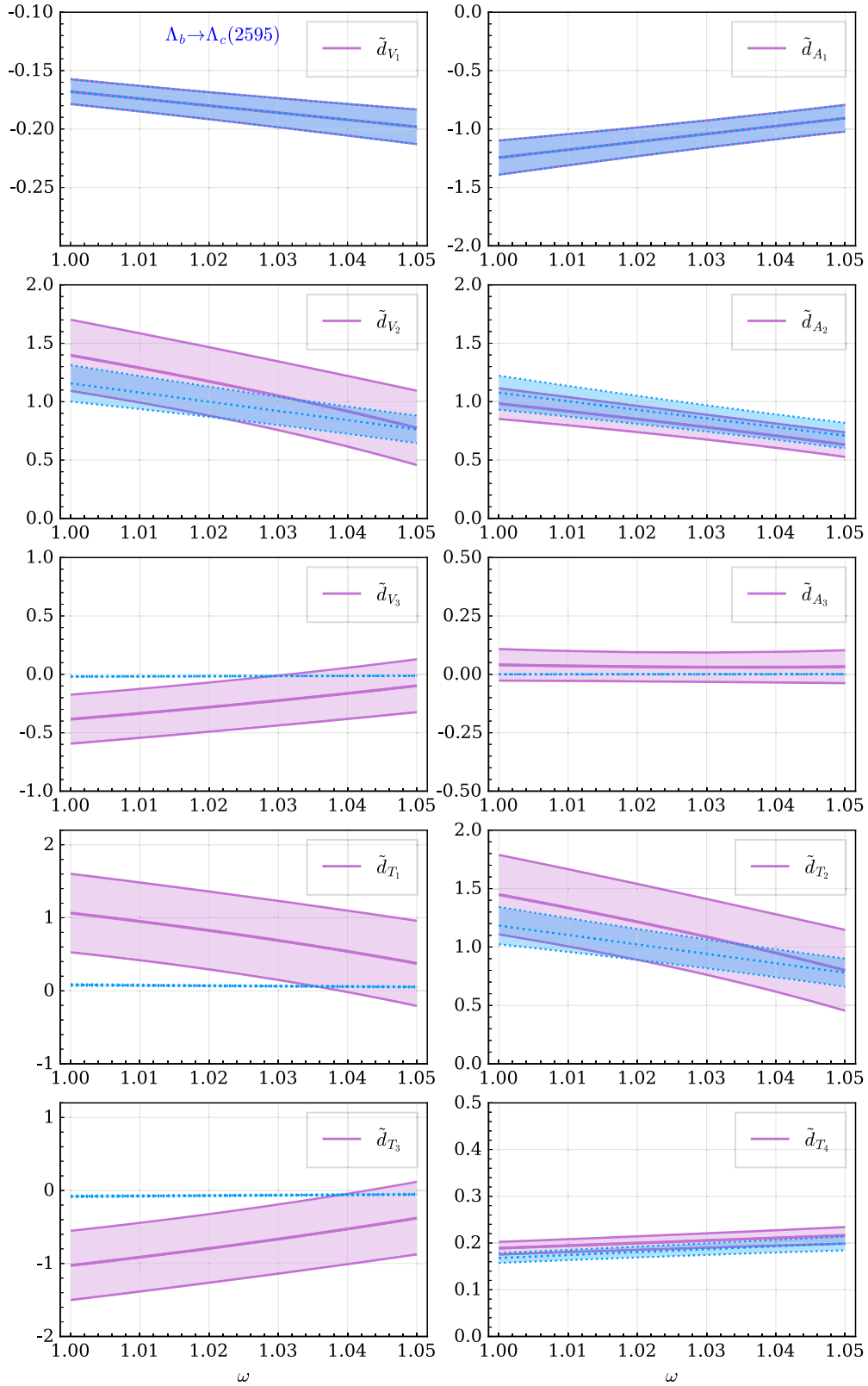


FIG. 1. Comparison between the LQCD [31] (purple uncertainty bands and solid curves) and the  $\mathcal{O}(\alpha_s, \Lambda_{\text{QCD}}/m_c)$  HQET [Eqs. (24) and (B1)] form factors for the  $\Lambda_b \rightarrow \Lambda_c(2595)^+$  transition, as a function of  $\omega$ . The HQET predictions are displayed by blue bands and dotted lines. The LQCD results are obtained using the relations given in Appendix A between the form factors displayed here and the helicity ones computed in Ref. [31].

shown in the plots. We do not show the scalar and pseudoscalar form factors ( $\tilde{d}_{S,P}$  and  $\tilde{l}_{S,P}$ ), since they were not computed in the LQCD simulation of Refs. [6,31]. They are given in Appendix A using their relation to the vector and axial-vector form factors obtained from the heavy quark equations of motion.

The comparison of the LQCD and  $\mathcal{O}(\alpha_s, \Lambda_{\text{QCD}}/m_c)$  HQET results for the helicity form factors, which are those directly obtained in the lattice calculation [6,31], are presented in Fig. 2 for  $\Lambda_b \rightarrow \Lambda_c(2595)^+$ , and Figs. 4 and 6 for  $\Lambda_b \rightarrow \Lambda_c(2625)^+$ . The comparison for the scalar and pseudoscalar form factors ( $\tilde{d}_{S,P}$  and  $\tilde{l}_{S,P}$ ) can be inferred from the results shown in these figures for  $f_0^{(J^P)}$  and  $g_0^{(J^P)}$ , cf. Eqs. (A1) and (A2).

For the  $\Lambda_b \rightarrow \Lambda_c(2595)^+$  transition, we see that LQCD and HQET agree in general within uncertainties. The largest discrepancies are found for the vector  $\tilde{d}_{V_3}$  and tensor  $\tilde{d}_{T_1}$  and  $\tilde{d}_{T_3}$  form factors. At this order within the HQET scheme, they are nonzero only because of the small radiative corrections, of the order of 0.02–0.03 as can be inferred from Table I in Appendix B, and they are hardly visible in the plots. Moreover, these form factors are poorly determined on the lattice and, in fact, the large uncertainties affecting them make these discrepancies of little significance. Note that the axial  $\tilde{d}_{A_3}$  form factor which also at this order of the HQET expansion gets only contributions from small short-distance terms, is accurately determined in Ref. [31], and it turns out to be compatible with zero in the whole  $\omega$  interval shown in the figure. The radiative corrections to  $\tilde{d}_{V_2}$  and  $\tilde{d}_{T_2}$  are somewhat larger than in the previous cases ( $\sim 5\%$ ) and slightly improve the agreement between LQCD and HQET predictions. The results in Fig. 2, where we pay attention to the helicity form factors directly determined in the LQCD simulation, confirm the quite reasonable comparison between LQCD and HQET predictions. The most significant discrepancy is found now for the axial  $g_0^{(\frac{1}{2}^-)}$  helicity form factor, which contributes to the axial  $\tilde{d}_{A_2}$  and  $\tilde{d}_{A_3}$ , where however LQCD and HQET predictions agree within errors. On the other hand, we do not appreciate significant discrepancies between both sets of predictions for the helicity form factors involved in the vector  $\tilde{d}_{V_3}$  and tensor  $\tilde{d}_{T_1}$  and  $\tilde{d}_{T_3}$ . Therefore, the origin of the differences noted above must be sought in the large cancellations responsible for these form factors being zero at order  $\mathcal{O}(\alpha_s, \Lambda_{\text{QCD}}/m_c)$ .

At first sight, the comparison of LQCD and  $\mathcal{O}(\alpha_s, \Lambda_{\text{QCD}}/m_c)$  HQET form factors for the  $\Lambda_b \rightarrow \Lambda_c(2625)^+$  decay does not look as satisfactory as that described above for  $\Lambda_b \rightarrow \Lambda_c(2595)^+$ , as one might infer from Figs. 3 and 5. In particular, the discrepancies are

clearly visible in  $\tilde{l}_{V_3}$ ,  $\tilde{l}_{V_4}$ ,  $\tilde{l}_{A_4}$ ,  $l_{T_5}$  and  $\tilde{l}_{T_6}$ , which are predicted to be zero at this order of the HQET expansion, except for the first one which gets a tiny short-distance contribution. We however note, the LQCD predictions of Ref. [31] for these form factors are compatible with typical values of order  $\mathcal{O}(\Lambda_{\text{QCD}}/m_b) \sim 0.1$ , except for the case of  $|\tilde{l}_{V_3}|$ , which takes notably higher values. As in the case of  $\tilde{d}_{V_3}$  for the  $\Lambda_b \rightarrow \Lambda_c(2595)^+$  mode, we also believe that the origin of the differences for  $\tilde{l}_{V_3}$  stems from some inaccuracies in the required large cancellations, among the  $f_0^{(\frac{3}{2}^-)}$ ,  $f_+^{(\frac{3}{2}^-)}$ ,  $f_\perp^{(\frac{3}{2}^-)}$  and  $f_{\perp'}^{(\frac{3}{2}^-)}$  helicity form factors, to make the leading and  $\mathcal{O}(\Lambda_{\text{QCD}}/m_c)$  contributions to this form factor vanish. The same helicity form factors, but in a different linear combination, appear also in  $\tilde{l}_{V_2}$ , for which some disagreement, near zero recoil, between LQCD and  $\mathcal{O}(\alpha_s, \Lambda_{\text{QCD}}/m_c)$  HQET predictions can be appreciated in Fig. 3. Paying now attention to the results in Figs. 4 and 6, we observe there are five dominant helicity transitions, those associated to  $f_0^{(\frac{3}{2}^-)}$ ,  $g_+^{(\frac{3}{2}^-)}$  and  $g_\perp^{(\frac{3}{2}^-)}$  for vector and axial-vector currents, and  $\tilde{h}_+^{(\frac{3}{2}^-)}$  and  $\tilde{h}_\perp^{(\frac{3}{2}^-)}$  for the tensor ones. Importantly, the  $\mathcal{O}(\alpha_s, \Lambda_{\text{QCD}}/m_c)$  HQET scheme provides a good reproduction of the LQCD results for these leading form factors.<sup>5</sup> The largest differences appear for  $f_0^{(\frac{3}{2}^-)}$ , where the central values of both schemes are separated by almost one sigma, which might explain the discrepancies pointed out above for  $\tilde{l}_{V_2}$  and  $\tilde{l}_{V_3}$ . The rest of the helicity form factors are very small, around a factor 20–40 smaller (in absolute value) than the five dominant ones mentioned above. Order  $\mathcal{O}(\Lambda_{\text{QCD}}/m_b)$  corrections to the HQET results or further systematic errors affecting the LQCD ones could change the predictions displayed in Figs. 4 and 6, and improve the apparent disagreement exhibited there for these subleading form factors.

Therefore, we conclude that the  $\mathcal{O}(\alpha_s, \Lambda_{\text{QCD}}/m_c)$  HQET scheme describes reasonably well the LQCD results, taking into account that the neglected HQET  $\mathcal{O}(\Lambda_{\text{QCD}}/m_b)$  sub-leading corrections or LQCD systematic uncertainties might be important in those cases where discrepancies are more apparent on a naive visual inspection of Figs. 3 and 5. The results of the next subsection will give further support to this general conclusion.

## B. HQSS form factors and differential decay rates

In this subsection, we try first to assess how well the  $\Lambda_c(2595)^+$  and  $\Lambda_c(2625)^+$  are described by a  $j_{\text{ldof}}^P = 1^-$

<sup>5</sup>We note that radiative corrections improve the agreement between both approaches for these helicity form factors, in particular for  $f_0^{(\frac{3}{2}^-)}$  ( $\propto \tilde{l}_S$ ),  $\tilde{h}_+^{(\frac{3}{2}^-)}$  and  $\tilde{h}_\perp^{(\frac{3}{2}^-)}$ .

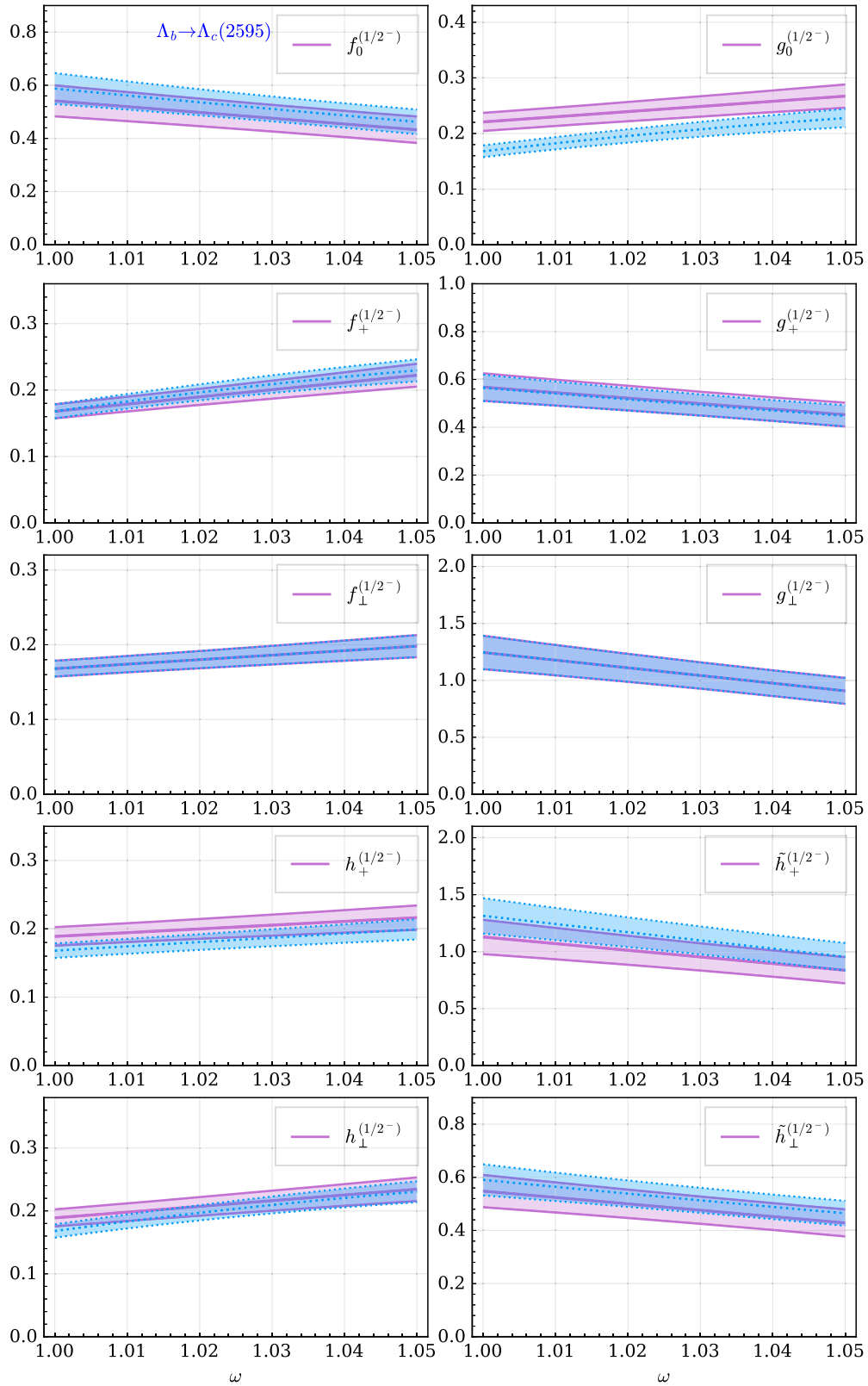


FIG. 2. Comparison of the  $\Lambda_b \rightarrow \Lambda_c(2595)^+$  LQCD (purple uncertainty bands and solid curves) and  $\mathcal{O}(\alpha_s, \Lambda_{\text{QCD}}/m_c)$  HQET results for the helicity form factors, which are those directly computed in Ref. [31], as a function of  $\omega$ . The HQET predictions are obtained by inverting the relations given in Appendix A, and using for the  $\tilde{d}_i$  form factors, the  $\mathcal{O}(\Lambda_{\text{QCD}}/m_c)$  expressions of Eq. (B1). The HQET predictions are displayed by blue bands and dotted lines.

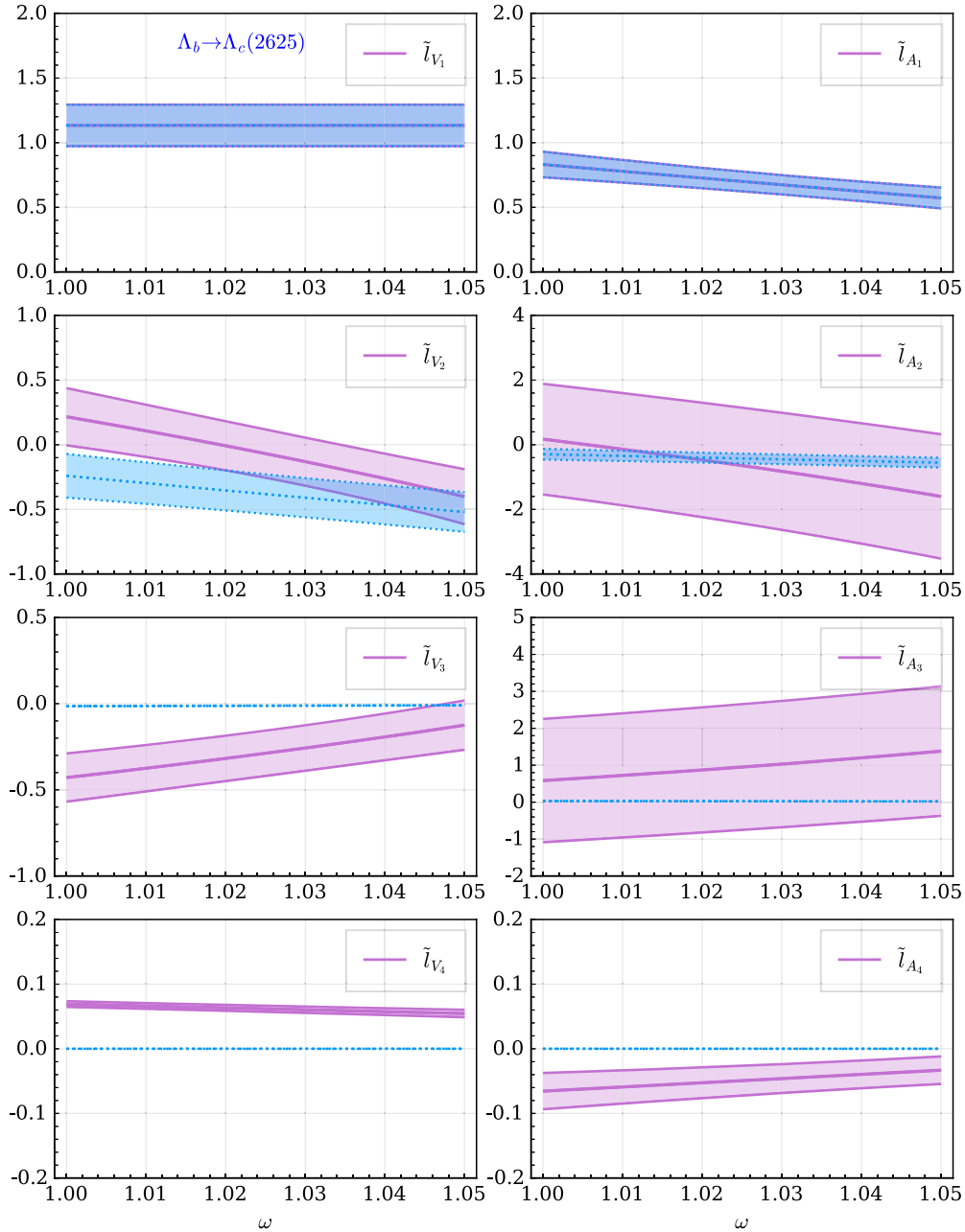


FIG. 3. Same as Fig. 1 for the  $\Lambda_b \rightarrow \Lambda_c(2625)^+$  vector and axial-vector form factors.

configuration for the  $1_{\text{dof}}$ . We discussed in Sec. III that  $\Delta_2(\omega) = \Omega_2(\omega) = 0$  in the heavy charm quark limit, and that in addition,  $\Delta_1(\omega) = \Omega_1(\omega) = \sigma(\omega)$  if the  $\Lambda_c(2595)^+$  and  $\Lambda_c(2625)^+$  are the members of the lowest-lying HQSS  $j_{\text{dof}}^P = 1^-$  doublet. Thus, the difference between the  $\Delta_1(\omega)$  and  $\Omega_1(\omega)$  should be of order  $\mathcal{O}(\Lambda_{\text{QCD}}/m_c)$ , while  $\Delta_2(\omega)$  and  $\Omega_2(\omega)$  are both of order  $\mathcal{O}(\Lambda_{\text{QCD}}/m_c)$ , and hence suppressed compared to the leading  $\Delta_1(\omega)$  and  $\Omega_1(\omega)$  functions, cf. (17). Note that the overall sign of the form factors for each decay mode depends on the phase conventions of the  $\Lambda_c^*$  states [6], and only the relative signs

among the form factors for a specific mode are well determined. The comparisons between the  $\Delta_{1,2}$  and  $\Omega_{1,2}$  IW functions, obtained from the LQCD results for the  $\tilde{d}_{V_1}, \tilde{d}_{A_1}, \tilde{l}_{V_1}$  and  $\tilde{l}_{A_2}$  form factors [Eq. (24)], are shown in Fig. 7. We see that the differences between  $\Delta_1$  and  $-\Omega_1$  are small compared to any,  $\Delta_1$  or  $\Omega_1$ , of these leading IW functions, and can be naturally attributed to  $\mathcal{O}(\Lambda_{\text{QCD}}/m_c)$  contributions. This gives some support, or at least does not contradict, that the  $\Lambda_c(2595)^+$  and  $\Lambda_c(2625)^+$  resonances might form the lowest-lying HQSS  $j_{\text{dof}}^P = 1^-$  doublet. Nevertheless, we would remind that in the LQCD

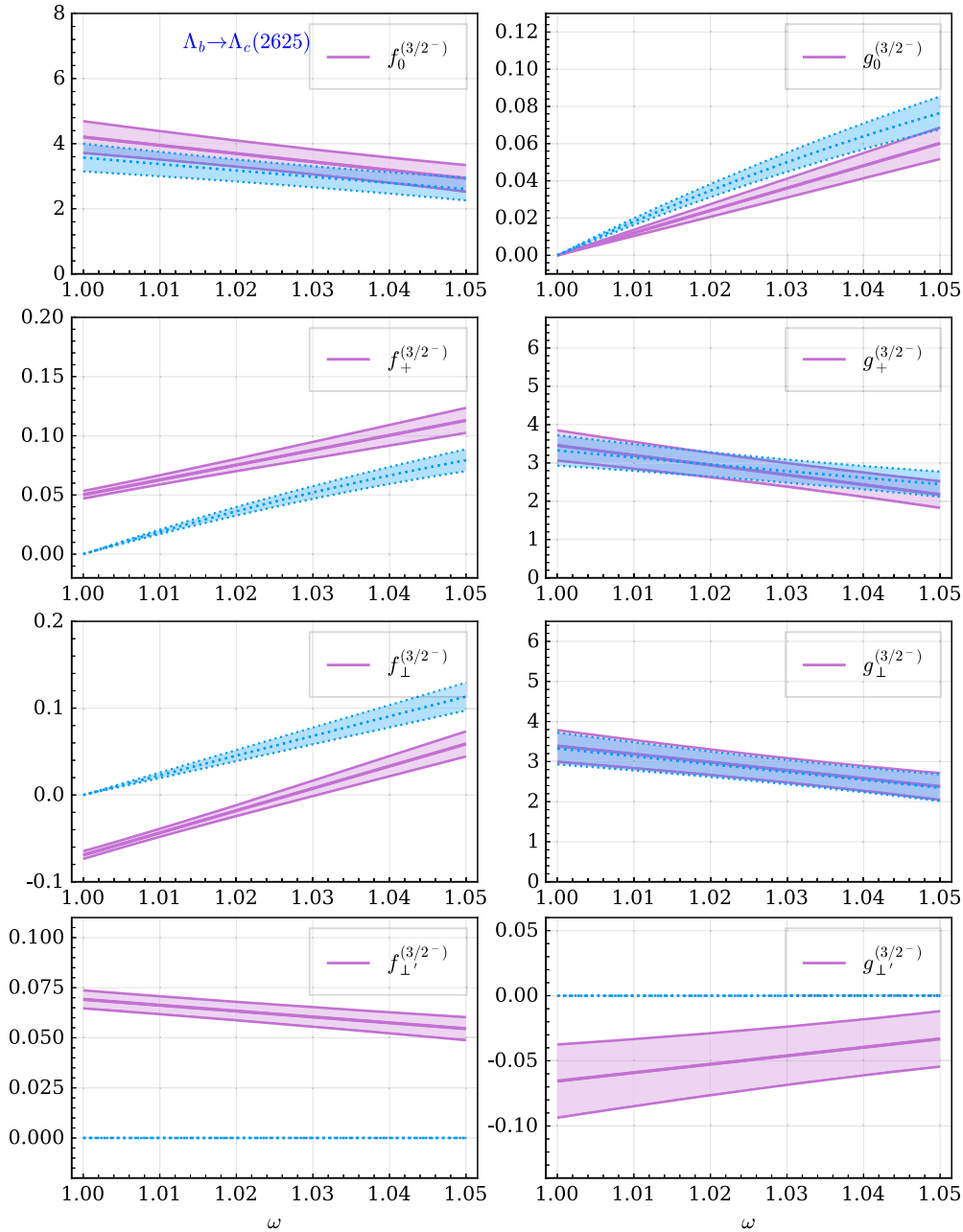
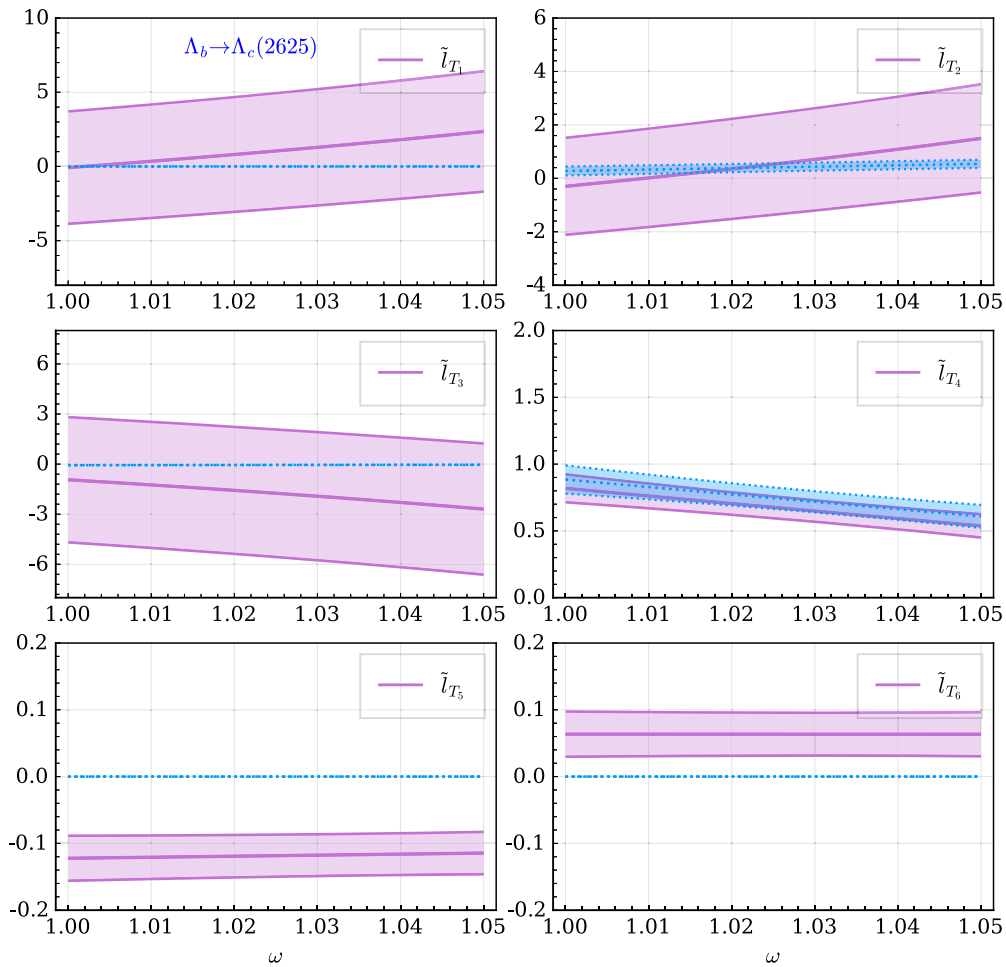


FIG. 4. Same as Fig. 2 for the  $\Lambda_b \rightarrow \Lambda_c(2625)^+$  scalar, pseudoscalar, vector and axial-vector helicity form factors.

simulation carried out in Refs. [6,31], the  $\Lambda_c^*$  states were described using three-quark interpolating fields. This should not create any bias for an unquenched simulation, since these operators should capture any baryon-meson ( $\Sigma_c^{(*)}\pi$ ) component in the QCD state, assuming a sufficiently large evolution time. The chiral-continuum extrapolations of the masses of the states excited on the lattice are [6]

$$\begin{aligned} m_{\Lambda_{c,1/2}^*} &= (2693 \pm 43_{\text{stat}} \pm 95_{\text{sys}}) \text{ MeV}, \\ m_{\Lambda_{c,3/2}^*} &= (2742 \pm 43_{\text{stat}} \pm 96_{\text{sys}}) \text{ MeV} \end{aligned} \quad (25)$$

which, though are consistent with the experimental values of  $m_{\Lambda_{c,1/2}^*} = 2592.25(28) \text{ MeV}$  and  $m_{\Lambda_{c,3/2}^*} = 2628.11(19) \text{ MeV}$  [47], are not accurate enough to disentangle the possible effects of the  $\Sigma_c\pi$  and  $\Sigma_c^*\pi$  thresholds located only a few MeV above the position of the physical resonances, especially in the case of the  $\Lambda_c(2595)^+$  and  $\Sigma_c\pi$  [27]. Therefore, the claim made in this latter reference that the  $\Lambda_c(2595)^+$  and  $\Lambda_c(2625)^+$  resonances are not HQSS partners cannot be discarded using the LQCD data studied here. In Ref. [27], the  $J^P = 3/2^-$  state is described mostly as a dressed three-quark state, whose origin is determined by a bare state [3],

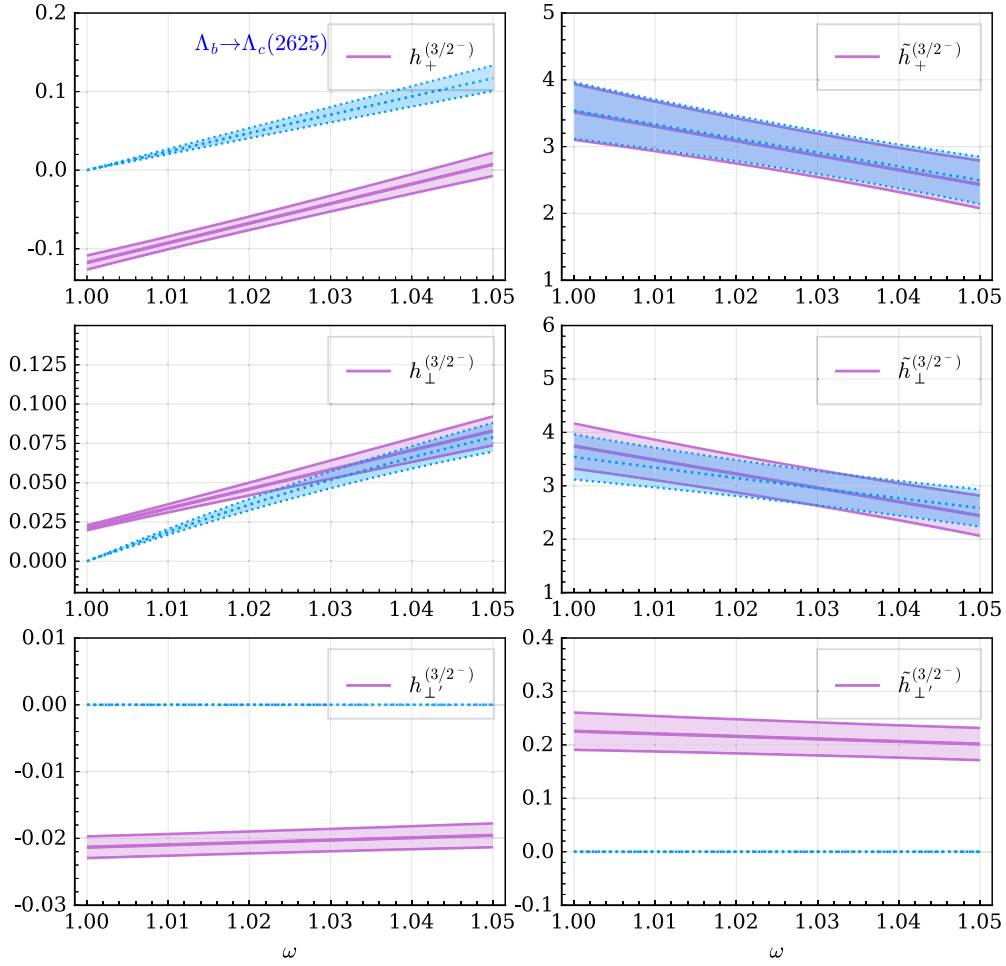
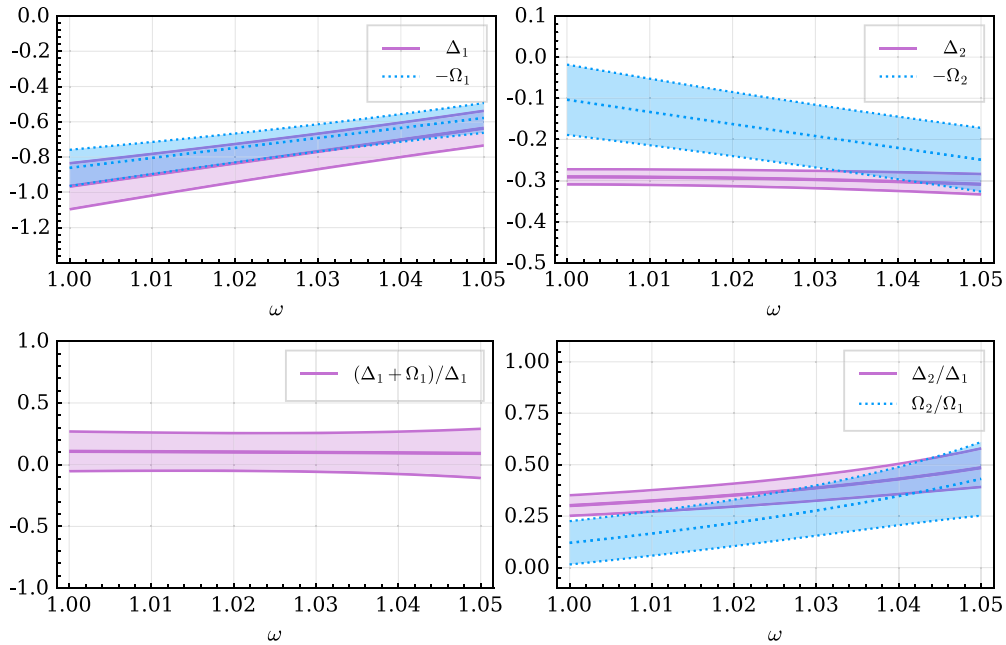
FIG. 5. Same as Fig. 1 for the  $\Lambda_b \rightarrow \Lambda_c(2625)^+$  tensor form factors.

predicted to lie very close to the mass of the resonance. The  $J^P = 1/2^-$  resonance seemed to have, however, a predominant molecular structure. This is, depending on the renormalization scheme, either because the  $\Lambda_c(2595)^+$  is the result of the chiral  $\Sigma_c\pi$  interaction [19,27], whose threshold is located much closer than the mass of the bare three-quark state, or because the  $1d_{\text{dof}}$  in its inner structure are coupled to the unnatural  $j_{\text{dof}}^P = 0^-$  quantum numbers which gives rise to a double-pole pattern for this resonance analog to that established for the  $\Lambda(1405)$  [17,18]. To shed light into this problem, it would require new LQCD simulations giving rise to more accurate determinations of the masses of the  $m_{\Lambda_{c,1/2}^*}$  and  $m_{\Lambda_{c,3/2}^*}$ , with precision better than the mass difference with the  $\Sigma_c\pi$  and  $\Sigma_c^*\pi$  thresholds, and using not only three-quark interpolating operators, but also other ones with larger overlaps to hadron-molecular degrees of freedom.

Coming back to Fig. 7, we observe that both  $\Delta_2$  and  $\Omega_2$  are also smaller (absolute value) than  $\Delta_1$  and  $\Omega_1$ ,

respectively, near zero recoil. Actually, the ratios  $\Delta_2/\Delta_1$  and  $\Omega_2/\Omega_1$  (right-bottom plot) have a typical size of order  $\mathcal{O}(\Lambda_{\text{QCD}}/m_c)$ . This supports the compatibility of the LQCD and  $\mathcal{O}(\alpha_s, \Lambda_{\text{QCD}}/m_c)$  HQET predictions for the form factors in the previous subsection. In the left plot of Fig. 8, we show the SM  $d\Gamma[\Lambda_b \rightarrow \Lambda_{c,J^P}^* \tau \bar{\nu}_\tau]/d\omega$  distributions, obtained both using the full set of the 14 LQCD form factors computed in Ref. [31] and the  $\mathcal{O}(\alpha_s, \Lambda_{\text{QCD}}/m_c)$  HQET expressions of Eqs. (20) and (21), which involve only the  $\Delta_{1,2}$  and  $\Omega_{1,2}$  functions determined in Eq. (24). We limit the comparison to the region of reliability of the LQCD form factors and find a good agreement, even more taking into account uncertainties, for the whole studied region.

On the other hand, we can see in Fig. 7 that in the vicinity of zero recoil,  $\Delta_2/\Delta_1$  is higher than  $\Omega_2/\Omega_1$ , reaching the former ratio values around 0.3–0.35. Moreover, since  $\Delta_2$  accounts for an S-wave term to the  $\Lambda_b \rightarrow \Lambda_{c,1/2}^*$  decay amplitude [see discussion of


 FIG. 6. Same as Fig. 2 for the  $\Lambda_b \rightarrow \Lambda_c(2625)^+$  tensor helicity form factors.

 FIG. 7. Comparison between the leading and subleading  $\Delta_{1,2}$  and  $\Omega_{1,2}$  functions, determined as specified in Eq. (24). Note that it would be necessary to include a relative phase between the states  $\Lambda_c(2595)^+$  and  $\Lambda_c(2625)^+$  to obtain  $\Delta_1$  and  $\Omega_1$  with the same sign.

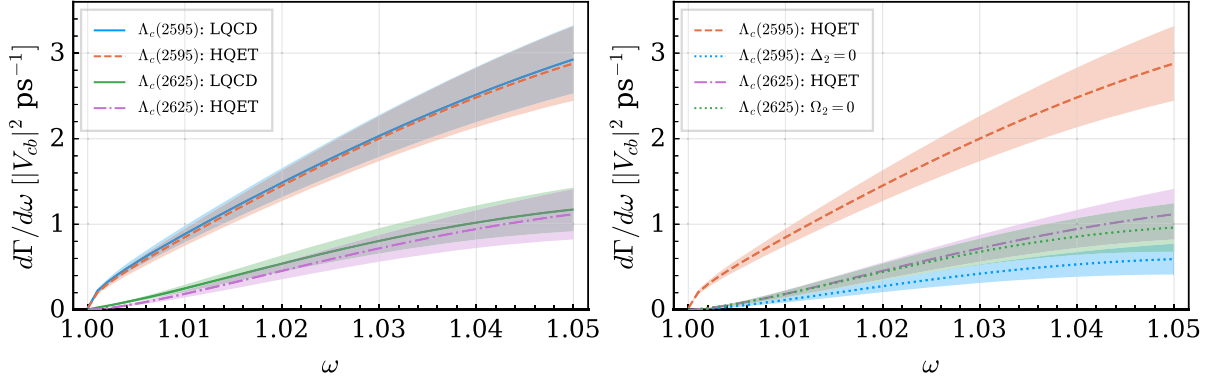


FIG. 8. SM  $d\Gamma[\Lambda_b \rightarrow \Lambda_c(2595)^+ \tau \bar{\nu}_\tau]/d\omega$  and  $d\Gamma[\Lambda_b \rightarrow \Lambda_c(2625)^+ \tau \bar{\nu}_\tau]/d\omega$  differential decay widths, as functions of  $\omega$ . We show distributions obtained using the full set of LQCD form factors computed in Ref. [31] (LQCD) and the expressions (HQET) of Eqs. (20) and (21), employing the  $\Delta_{1,2}$  and  $\Omega_{1,2}$  functions determined in Eq. (24). For the latter scheme, in the right panel, we compare the full  $\mathcal{O}(\alpha_s, \Lambda_{\text{QCD}}/m_c)$  HQET results with those obtained after setting to zero the subleading  $\Delta_2$  and  $\Omega_2$  functions.

Eq. (22)], which becomes dominant close to  $\omega = 1$ , we see in the right-bottom panel of Fig. 8 that this subleading IW function has an enormous numerical impact in the  $\Lambda_b \rightarrow \Lambda_c(2595)^+$  differential decay distribution, and its contribution becomes totally dominant. This result confirms the findings of Refs. [1,25], obtained using the soliton model derived in Ref. [1], where the large size of these finite charm quark mass HQSS breaking terms on the  $\Lambda_c(2595)^+$  differential decay distribution was first pointed out (see for instance Fig. 2 of Ref. [25]). In sharp contrast, the effects on the  $\Lambda_c(2625)^+$  distribution of the subleading  $\Omega_2$  function are small below  $\omega = 1.05$  (right panel of Fig. 8).

From the above discussion, we naturally find an explanation for large deviations, near zero recoil, of the  $\frac{d\Gamma[\Lambda_b \rightarrow \Lambda_{c,1/2}^*]/d\omega}{d\Gamma[\Lambda_b \rightarrow \Lambda_{c,3/2}^*]/d\omega}$  ratio from the value of 1/2 predicted in the  $m_Q \rightarrow \infty$  limit, assuming that the  $\Lambda_{c,1/2}^*$  and  $\Lambda_{c,3/2}^*$  are the two members of the  $j_{\text{ldof}}^P = 1^-$  HQSS doublet. Actually, this ratio at  $\omega = 1.05$  takes values around 2.5 and much larger ones in the near-zero recoil regime. This tension between LQCD data and the HQET predictions triggered the claim in Refs. [7,31] of unexpectedly large HQSS-violating terms, with potentially large  $1/m_c^2$  corrections, near zero recoil.<sup>6</sup> We assign here these huge HQSS breaking corrections, not necessarily just to big values of the  $\Delta_2(\omega)/\Delta_1(\omega)$  ratio of leading to subleading IW functions, but also to the fact

<sup>6</sup>The authors of Refs. [7,31] pointed out that such large HQSS-violating terms cannot persist uniformly over the full recoil spectrum, as they would be incompatible with the measurement of the ratio of total decay rates in the muon mode [48]

$$\frac{\Gamma[\Lambda_b \rightarrow \Lambda_{c,1/2}^* \mu \bar{\nu}_\mu]}{\Gamma[\Lambda_b \rightarrow \Lambda_{c,3/2}^* \mu \bar{\nu}_\mu]} = 0.6 \pm 0.2_{-0.3}^{+0.5}. \quad (26)$$

that the  $\Delta_2(\omega)$  form factor accounts for an S-wave term to the  $\Lambda_b \rightarrow \Lambda_{c,1/2}^*$  decay amplitude, while after having not considered  $\mathcal{O}(\Lambda_{\text{QCD}}/m_b)$  corrections, the  $\Lambda_b \rightarrow \Lambda_{c,3/2}^*$  semileptonic decay proceeds necessarily at least in P wave, and it is therefore suppressed by a factor  $(\omega^2 - 1)^{3/2}$  at zero recoil.

One might wonder if the S-wave term, proportional to  $\tilde{l}_{V_4}$ , which we have neglected in  $\Lambda_b \rightarrow \Lambda_{c,3/2}^*$  decay, can change this conclusion. From the general analytical expressions given in Appendix B of Ref. [41], we find

$$\begin{aligned} & \left. \frac{d\Gamma[\Lambda_b \rightarrow \Lambda_{c,1/2}^* \ell \bar{\nu}_\ell]/d\omega}{d\Gamma[\Lambda_b \rightarrow \Lambda_{c,3/2}^* \ell \bar{\nu}_\ell]/d\omega} \right|_{\omega=1} \\ &= \frac{3\tilde{d}_{V_1}^2(1)}{2\tilde{l}_{V_4}^2(1)} \left[ 1 + \frac{(\tilde{d}_{A_1} + \tilde{d}_{A_2} + \tilde{d}_{A_3})^2/\tilde{d}_{V_1}^2}{1 + 2\left(\frac{m_{\Lambda_b} - m_{\Lambda_c^*}}{m_\ell}\right)^2} \right]_{\omega=1} \\ &\geq \frac{3\tilde{d}_{V_1}^2(1)}{2\tilde{l}_{V_4}^2(1)} \sim \frac{9m_b^2}{8m_c^2} \left(1 - \frac{m_c}{3m_b}\right)^2 > 10, \end{aligned} \quad (27)$$

where in the last equality we have made use of Eqs. (27c) and (28f) of Ref. [7] to estimate the  $\tilde{d}_{V_1}(1)/\tilde{l}_{V_4}(1)$  ratio. The result above does not modify, but it instead reinforces, the theoretical expectation of finding large deviations from 1/2 for the ratio of differential decay rates in the vicinity of zero recoil.<sup>7</sup> When  $\Delta_2$  and  $\Omega_2$  are set to zero, we recover within errors the value of 1/2 for the ratio of

<sup>7</sup>Note that from Eq. (28f) of Ref. [7],  $\tilde{l}_{V_4}(1) = 2(\bar{\Lambda}' - \bar{\Lambda})\sigma(1)/(2m_b) \sim 0.06\sigma(1)$ , which is in good agreement with the LQCD results depicted here in the left-bottom plot of Fig. 3. This nonzero value for  $\tilde{l}_{V_4}(1)$  explains the differences observed in Fig. 8 between the  $1/2^+ \rightarrow 3/2^-$  distributions obtained using the full set of LQCD form factors and the  $\mathcal{O}(\alpha_s, \Lambda_{\text{QCD}}/m_c)$  HQET expressions derived in our approach.

differential decay widths, see right plot of Fig. 8. This is so because, taking into account uncertainties,  $\Delta_1(\omega) \sim -\Omega_1(\omega)$  even in the presence of  $\mathcal{O}(\Lambda_{\text{QCD}}/m_c)$  corrections to these leading IW functions (see top left panel of Fig. 7). This is in accordance with the  $\Lambda_c(2595)^+$  and  $\Lambda_c(2625)^+$  being HQSS partners.

As a final comment, we just mention that we have also carried out the present analysis using the first LQCD results obtained in [6], where the relations among the different form factors at zero recoil which follow from rotational symmetry [31] were not imposed. The results for the helicity form factors and differential rates are similar to those obtained from the updated LQCD simulation and presented above. However, some of the  $\tilde{d}_i$  and  $\tilde{l}_i$  (specifically,  $\tilde{d}_{V_{i=2,3}}$ ,  $\tilde{d}_{T_{i=1,2,3}}$  and  $\tilde{l}_{V_{i=1,2,3}}$ ,  $\tilde{l}_{A_{i=2,3}}$ ,  $\tilde{l}_{T_{i=1,2,3}}$ ) form factors and the subleading  $\Omega_2$  IW do not converge at  $\omega = 1$ , which introduces large uncertainties near the zero-recoil point.

## V. SUMMARY

We have used the  $\mathcal{O}(\Lambda_{\text{QCD}}/m_c)$  HQET scheme derived in Ref. [25], in which invariance under rotations of the spin of the  $b$  quark is preserved, to study the matrix elements of the scalar, pseudoscalar, vector, axial-vector and tensor currents between the  $\Lambda_b$  ground state and the odd parity charm  $\Lambda_c(2595)^+$  and  $\Lambda_c(2625)^+$  resonances. In this work, we have additionally included short-distance radiative corrections, and thus only  $\mathcal{O}(\Lambda_{\text{QCD}}/m_b)$  corrections are neglected. There are only four independent functions  $\Delta_{1,2}(\omega)$  and  $\Omega_{1,2}(\omega)$  for the  $\Lambda_b \rightarrow \Lambda_{c,1/2}^*$  and  $\Lambda_b \rightarrow \Lambda_{c,3/2}^*$  semi-leptonic decays, respectively, which are determined from a recent LQCD computation of the corresponding helicity form factors [6,31]. We have shown that in the near-zero recoil regime, this  $\mathcal{O}(\alpha_s, \Lambda_{\text{QCD}}/m_c)$  HQET scheme describes reasonably well, taking into account systematic uncertainties, the results for the total of 24 form factors obtained in the LQCD studies of Refs. [6,31].

We have found that the differences between  $\Delta_1$  and  $-\Omega_1$  are small compared to any,  $\Delta_1$  or  $\Omega_1$ , of these leading IW functions, and can be naturally attributed to  $\mathcal{O}(\Lambda_{\text{QCD}}/m_c)$  contributions. This gives some support, or at least does not contradict, to the scenario in which the  $\Lambda_c(2595)^+$  and  $\Lambda_c(2625)^+$  resonances might form the

lowest-lying HQSS  $j_{\text{dof}}^P = 1^-$  doublet. However, we have argued that the available LQCD description of these two resonances is not accurate enough to disentangle the possible effects of the  $\Sigma_c\pi$  and  $\Sigma_c^*\pi$  thresholds, located only a few MeV above the position of these excited states, especially in the case of the  $\Lambda_c(2595)^+$  and  $\Sigma_c\pi$  [27]. The claim made in this latter reference that the  $\Lambda_c(2595)^+$  and  $\Lambda_c(2625)^+$  resonances are not HQSS partners cannot be discarded using the LQCD data studied here. To clarify this problem, new and more precise LQCD simulations capable of elucidating the role played by the  $\Sigma_c\pi$  and  $\Sigma_c^*\pi$  channels and that make use, not only of three-quark interpolating fields, but also of other operators with larger overlaps to hadron-molecular degrees of freedom will be required.

Finally, we have naturally given an explanation to the large deviations, near zero recoil, of the  $\frac{d\Gamma[\Lambda_b \rightarrow \Lambda_{c,1/2}^*]/d\omega}{d\Gamma[\Lambda_b \rightarrow \Lambda_{c,3/2}^*]/d\omega}$  ratio from 1/2, value predicted in the  $m_Q \rightarrow \infty$  limit assuming that the  $\Lambda_{c,1/2}^*$  and  $\Lambda_{c,3/2}^*$  are the two members of the  $j_{\text{dof}}^P = 1^-$  HQSS doublet. We have related these huge HQSS breaking corrections, not necessarily to just big values of the  $\Delta_2(\omega)/\Delta_1(\omega)$  ratio of subleading to leading IW functions, but also to the S-wave character of the contributions to the  $\Lambda_b \rightarrow \Lambda_{c,1/2}^*$  decay amplitude driven by  $\Delta_2(\omega)$ .

## ACKNOWLEDGMENTS

We are grateful to J.M. Flynn for helpful discussions. This research has been supported by the Spanish Ministerio de Ciencia e Innovación (MICINN) and the European Regional Development Fund (ERDF) under Contracts No. PID2020–112777GB-I00 and No. PID2019–105439GB-C22, the EU STRONG-2020 project under the Program No. H2020-INFRAIA-2018-1, Grant Agreement No. 824093 and by Generalitat Valenciana under Contract No. PROMETEO/2020/023.

## APPENDIX A: LQCD FORM FACTORS

The relations between the form factors in Eqs. (1) and (2) and the LQCD ones computed in Ref. [31] are for  $\Lambda_b \rightarrow \Lambda_c(2595)^+$ ,

$$\begin{aligned}
\tilde{d}_S &= f_0^{(\frac{1}{2}^-)} \frac{m_{\Lambda_b} + m_{\Lambda_{c,1/2}^*}}{m_b - m_c}, \\
\tilde{d}_P &= g_0^{(\frac{1}{2}^-)} \frac{m_{\Lambda_b} - m_{\Lambda_{c,1/2}^*}}{m_b + m_c}, \\
\tilde{d}_{V_1} &= -f_{\perp}^{(\frac{1}{2}^-)}, \\
\tilde{d}_{V_2} &= m_{\Lambda_b} \left[ \frac{m_{\Lambda_b} + m_{\Lambda_{c,1/2}^*}}{q^2} f_0^{(\frac{1}{2}^-)} + \frac{m_{\Lambda_b} - m_{\Lambda_{c,1/2}^*}}{s_-} \left( 1 - \frac{m_{\Lambda_b}^2 - m_{\Lambda_{c,1/2}^*}^2}{q^2} \right) f_+^{(\frac{1}{2}^-)} + \frac{2m_{\Lambda_{c,1/2}^*}}{s_-} f_{\perp}^{(\frac{1}{2}^-)} \right], \\
\tilde{d}_{V_3} &= m_{\Lambda_{c,1/2}^*} \left[ -\frac{m_{\Lambda_b} + m_{\Lambda_{c,1/2}^*}}{q^2} f_0^{(\frac{1}{2}^-)} + \frac{m_{\Lambda_b} - m_{\Lambda_{c,1/2}^*}}{s_-} \left( 1 + \frac{m_{\Lambda_b}^2 - m_{\Lambda_{c,1/2}^*}^2}{q^2} \right) f_+^{(\frac{1}{2}^-)} - \frac{2m_{\Lambda_b}}{s_-} f_{\perp}^{(\frac{1}{2}^-)} \right], \\
\tilde{d}_{A_1} &= -g_{\perp}^{(\frac{1}{2}^-)}, \\
\tilde{d}_{A_2} &= -m_{\Lambda_b} \left[ \frac{m_{\Lambda_b} - m_{\Lambda_{c,1/2}^*}}{q^2} g_0^{(\frac{1}{2}^-)} + \frac{m_{\Lambda_b} + m_{\Lambda_{c,1/2}^*}}{s_+} \left( 1 - \frac{m_{\Lambda_b}^2 - m_{\Lambda_{c,1/2}^*}^2}{q^2} \right) g_+^{(\frac{1}{2}^-)} - \frac{2m_{\Lambda_{c,1/2}^*}}{s_+} g_{\perp}^{(\frac{1}{2}^-)} \right], \\
\tilde{d}_{A_3} &= m_{\Lambda_{c,1/2}^*} \left[ \frac{m_{\Lambda_b} - m_{\Lambda_{c,1/2}^*}}{q^2} g_0^{(\frac{1}{2}^-)} - \frac{m_{\Lambda_b} + m_{\Lambda_{c,1/2}^*}}{s_+} \left( 1 + \frac{m_{\Lambda_b}^2 - m_{\Lambda_{c,1/2}^*}^2}{q^2} \right) g_+^{(\frac{1}{2}^-)} + \frac{2m_{\Lambda_b}}{s_+} g_{\perp}^{(\frac{1}{2}^-)} \right], \\
\tilde{d}_{T_1} &= 2m_{\Lambda_b}^2 \left( \frac{1}{s_-} h_+^{(\frac{1}{2}^-)} - \frac{(m_{\Lambda_b} - m_{\Lambda_{c,1/2}^*})^2}{q^2 s_-} h_{\perp}^{(\frac{1}{2}^-)} - \frac{1}{s_+} \tilde{h}_+^{(\frac{1}{2}^-)} + \frac{(m_{\Lambda_b} + m_{\Lambda_{c,1/2}^*})^2}{q^2 s_+} \tilde{h}_{\perp}^{(\frac{1}{2}^-)} \right), \\
\tilde{d}_{T_2} &= 2m_{\Lambda_b} \left( \frac{m_{\Lambda_{c,1/2}^*}}{s_-} h_+^{(\frac{1}{2}^-)} - \frac{(m_{\Lambda_b} - m_{\Lambda_{c,1/2}^*})(m_{\Lambda_b}^2 - m_{\Lambda_{c,1/2}^*}^2 - q^2)}{2q^2 s_-} h_{\perp}^{(\frac{1}{2}^-)} + \frac{m_{\Lambda_b} + m_{\Lambda_{c,1/2}^*}}{2q^2} \tilde{h}_{\perp}^{(\frac{1}{2}^-)} \right), \\
\tilde{d}_{T_3} &= 2m_{\Lambda_b} \left( -\frac{m_{\Lambda_b}}{s_-} h_+^{(\frac{1}{2}^-)} + \frac{(m_{\Lambda_b} - m_{\Lambda_{c,1/2}^*})(m_{\Lambda_b}^2 - m_{\Lambda_{c,1/2}^*}^2 + q^2)}{2q^2 s_-} h_{\perp}^{(\frac{1}{2}^-)} - \frac{m_{\Lambda_b} + m_{\Lambda_{c,1/2}^*}}{2q^2} \tilde{h}_{\perp}^{(\frac{1}{2}^-)} \right), \\
\tilde{d}_{T_4} &= h_+^{(\frac{1}{2}^-)},
\end{aligned} \tag{A1}$$

and for  $\Lambda_b \rightarrow \Lambda_c(2625)^+$ ,

$$\begin{aligned}
\tilde{l}_S &= f_0^{(\frac{3}{2}^-)} \frac{m_{\Lambda_b} m_{\Lambda_{c,3/2}^*}}{s_+} \frac{m_{\Lambda_b} - m_{\Lambda_{c,3/2}^*}}{m_b - m_c}, \\
\tilde{l}_P &= g_0^{(\frac{3}{2}^-)} \frac{m_{\Lambda_b} m_{\Lambda_{c,3/2}^*}}{s_-} \frac{m_{\Lambda_b} + m_{\Lambda_{c,3/2}^*}}{m_b + m_c}, \\
\tilde{l}_{V_1} &= \frac{m_{\Lambda_b} m_{\Lambda_{c,3/2}^*}}{s_-} (f_{\perp}^{(\frac{3}{2}^-)} + f_{\perp'}^{(\frac{3}{2}^-)}), \\
\tilde{l}_{V_2} &= \frac{m_{\Lambda_b}^2 m_{\Lambda_{c,3/2}^*}}{s_+ s_-} \left[ f_0^{(\frac{3}{2}^-)} \frac{(m_{\Lambda_b} - m_{\Lambda_{c,3/2}^*}) s_-}{q^2} + f_+^{(\frac{3}{2}^-)} (m_{\Lambda_b} + m_{\Lambda_{c,3/2}^*}) \left( 1 - \frac{m_{\Lambda_b}^2 - m_{\Lambda_{c,3/2}^*}^2}{q^2} \right) - 2m_{\Lambda_{c,3/2}^*} f_{\perp}^{(\frac{3}{2}^-)} + 2m_{\Lambda_{c,3/2}^*} f_{\perp'}^{(\frac{3}{2}^-)} \right], \\
\tilde{l}_{V_3} &= \frac{m_{\Lambda_b} m_{\Lambda_{c,3/2}^*}^2}{s_+ s_-} \left[ -f_0^{(\frac{3}{2}^-)} \frac{(m_{\Lambda_b} - m_{\Lambda_{c,3/2}^*}) s_-}{q^2} + f_+^{(\frac{3}{2}^-)} (m_{\Lambda_b} + m_{\Lambda_{c,3/2}^*}) \left( 1 + \frac{m_{\Lambda_b}^2 - m_{\Lambda_{c,3/2}^*}^2}{q^2} \right) - 2m_{\Lambda_b} f_{\perp}^{(\frac{3}{2}^-)} + 2 \left( m_{\Lambda_b} - \frac{s_+}{m_{\Lambda_{c,3/2}^*}} \right) f_{\perp'}^{(\frac{3}{2}^-)} \right], \\
\tilde{l}_{V_4} &= f_{\perp'}^{(\frac{3}{2}^-)}, \\
\tilde{l}_{A_1} &= \frac{m_{\Lambda_b} m_{\Lambda_{c,3/2}^*}}{s_+} (g_{\perp}^{(\frac{3}{2}^-)} + g_{\perp'}^{(\frac{3}{2}^-)}), \\
\tilde{l}_{A_2} &= \frac{m_{\Lambda_b}^2 m_{\Lambda_{c,3/2}^*}}{s_+ s_-} \left[ -\frac{(m_{\Lambda_b} + m_{\Lambda_{c,3/2}^*}) s_+}{q^2} g_0^{(\frac{3}{2}^-)} + \frac{(m_{\Lambda_b} - m_{\Lambda_{c,3/2}^*})(m_{\Lambda_b}^2 - m_{\Lambda_{c,3/2}^*}^2 - q^2)}{q^2} g_+^{(\frac{3}{2}^-)} - 2m_{\Lambda_{c,3/2}^*} g_{\perp}^{(\frac{3}{2}^-)} + 2m_{\Lambda_{c,3/2}^*} g_{\perp'}^{(\frac{3}{2}^-)} \right],
\end{aligned}$$

$$\begin{aligned}
\tilde{l}_{A_3} &= \frac{m_{\Lambda_b} m_{\Lambda_{c,3/2}^*}^2}{s_+ s_-} \left[ \frac{(m_{\Lambda_b} + m_{\Lambda_{c,3/2}^*}) s_+}{q^2} g_0^{(\frac{3}{2}^-)} - \frac{(m_{\Lambda_b} - m_{\Lambda_{c,3/2}^*})(m_{\Lambda_b}^2 - m_{\Lambda_{c,3/2}^*}^2 + q^2)}{q^2} g_+^{(\frac{3}{2}^-)} + 2m_{\Lambda_b} g_{\perp}^{(\frac{3}{2}^-)} - 2 \left( m_{\Lambda_b} + \frac{s_-}{m_{\Lambda_{c,3/2}^*}} \right) g_{\perp'}^{(\frac{3}{2}^-)} \right], \\
\tilde{l}_{A_4} &= g_{\perp'}^{(\frac{3}{2}^-)}, \\
\tilde{l}_{T_1} &= \frac{2m_{\Lambda_b}^3}{q^2 s_- s_+} (m_{\Lambda_{c,3/2}^*} [(m_{\Lambda_b} + m_{\Lambda_{c,3/2}^*})^2 h_{\perp}^{(\frac{3}{2}^-)} + q^2 (\tilde{h}_+^{(\frac{3}{2}^-)} - h_+^{(\frac{3}{2}^-)}) - (m_{\Lambda_b} - m_{\Lambda_{c,3/2}^*})^2 \tilde{h}_{\perp}^{(\frac{3}{2}^-)}] \\
&\quad + h_{\perp'}^{(\frac{3}{2}^-)} (m_{\Lambda_b} + m_{\Lambda_{c,3/2}^*}) (m_{\Lambda_b}^2 + m_{\Lambda_b} m_{\Lambda_{c,3/2}^*} - q^2) + (m_{\Lambda_b} - m_{\Lambda_{c,3/2}^*}) (m_{\Lambda_b}^2 - m_{\Lambda_b} m_{\Lambda_{c,3/2}^*} - q^2) \tilde{h}_{\perp'}^{(\frac{3}{2}^-)}), \\
\tilde{l}_{T_2} &= \frac{m_{\Lambda_b}^2 m_{\Lambda_{c,3/2}^*}}{q^2 s_- s_+} (s_+ (m_{\Lambda_b} + m_{\Lambda_{c,3/2}^*}) (h_{\perp}^{(\frac{3}{2}^-)} + h_{\perp'}^{(\frac{3}{2}^-)}) + (m_{\Lambda_b} - m_{\Lambda_{c,3/2}^*}) (m_{\Lambda_b}^2 - m_{\Lambda_{c,3/2}^*}^2 - q^2) (\tilde{h}_{\perp'}^{(\frac{3}{2}^-)} - \tilde{h}_{\perp}^{(\frac{3}{2}^-)}) + 2m_{\Lambda_{c,3/2}^*} q^2 \tilde{h}_+^{(\frac{3}{2}^-)}), \\
\end{aligned} \tag{A2}$$

$$\begin{aligned}
\tilde{l}_{T_3} &= -\frac{m_{\Lambda_b}}{q^2 s_- s_+} (s_+ [m_{\Lambda_b}^3 - q^2 (m_{\Lambda_b} + m_{\Lambda_{c,3/2}^*}) + m_{\Lambda_{c,3/2}^*}^3] h_{\perp'}^{(\frac{3}{2}^-)} + m_{\Lambda_b} m_{\Lambda_{c,3/2}^*} [s_+ (m_{\Lambda_b} + m_{\Lambda_{c,3/2}^*}) h_{\perp}^{(\frac{3}{2}^-)} \\
&\quad - (m_{\Lambda_b} - m_{\Lambda_{c,3/2}^*}) (m_{\Lambda_b}^2 - m_{\Lambda_{c,3/2}^*}^2 + q^2) \tilde{h}_{\perp}^{(\frac{3}{2}^-)} + 2m_{\Lambda_b} q^2 \tilde{h}_+^{(\frac{3}{2}^-)}] \\
&\quad + (m_{\Lambda_b} - m_{\Lambda_{c,3/2}^*}) (m_{\Lambda_b}^2 - m_{\Lambda_b} m_{\Lambda_{c,3/2}^*} + m_{\Lambda_{c,3/2}^*}^2 - q^2) (m_{\Lambda_b}^2 - m_{\Lambda_{c,3/2}^*}^2 + q^2) \tilde{h}_{\perp'}^{(\frac{3}{2}^-)}), \\
\tilde{l}_{T_4} &= -\frac{m_{\Lambda_{c,3/2}^*}}{q^2 s_+} (s_+ (m_{\Lambda_b} + m_{\Lambda_{c,3/2}^*}) h_{\perp'}^{(\frac{3}{2}^-)} + (m_{\Lambda_b} - m_{\Lambda_{c,3/2}^*}) (m_{\Lambda_b}^2 - m_{\Lambda_{c,3/2}^*}^2 + q^2) \tilde{h}_{\perp'}^{(\frac{3}{2}^-)} - m_{\Lambda_b} q^2 \tilde{h}_+^{(\frac{3}{2}^-)}) \\
\tilde{l}_{T_5} &= -\frac{s_+ h_{\perp'}^{(\frac{3}{2}^-)} (m_{\Lambda_b} + m_{\Lambda_{c,3/2}^*}) + (m_{\Lambda_b} - m_{\Lambda_{c,3/2}^*}) (m_{\Lambda_b}^2 - m_{\Lambda_{c,3/2}^*}^2 + q^2) \tilde{h}_{\perp'}^{(\frac{3}{2}^-)}}{2m_{\Lambda_b} q^2}, \\
\tilde{l}_{T_6} &= \frac{h_{\perp'}^{(\frac{3}{2}^-)} (m_{\Lambda_b} + m_{\Lambda_{c,3/2}^*})^2 + (m_{\Lambda_b} - m_{\Lambda_{c,3/2}^*})^2 \tilde{h}_{\perp'}^{(\frac{3}{2}^-)}}{q^2}, \\
\end{aligned} \tag{A3}$$

where  $q = p - p'$ ,  $s_{\pm} = (m_{\Lambda_b} \pm m_{\Lambda_c^*})^2 - q^2$  and  $m_b(m_c)$  is the mass of the  $b(c)$  quark. The equations of motion of the heavy quarks have been used to derive the scalar and pseudoscalar form factors.

## APPENDIX B: HQET PREDICTIONS FOR THE FORM FACTORS

The nonvanishing form factors in HQET up to  $\mathcal{O}(\alpha_s, \Lambda_{\text{QCD}}/m_c)$  read

$$\begin{aligned}
\tilde{d}_S &= -\frac{1}{\sqrt{3}} [(1 + \omega)(1 + C_S \hat{\alpha}_s) \Delta_1 + \Delta_2], & \tilde{d}_P &= -\frac{1}{\sqrt{3}} [(\omega - 1)(1 + C_P \hat{\alpha}_s) \Delta_1 + \Delta_2], \\
\tilde{d}_{V_1} &= \frac{1}{\sqrt{3}} [(\omega - 1)(1 + C_{V_1} \hat{\alpha}_s) \Delta_1 + \Delta_2], & \tilde{d}_{V_2} &= -\frac{2 + (2C_{V_1} + C_{V_2}(\omega + 1)) \hat{\alpha}_s}{\sqrt{3}} \Delta_1, & \tilde{d}_{V_3} &= -\frac{1 + \omega}{\sqrt{3}} C_{V_3} \hat{\alpha}_s \Delta_1, \\
\tilde{d}_{A_1} &= \frac{1}{\sqrt{3}} [(\omega + 1)(1 + C_{A_1} \hat{\alpha}_s) \Delta_1 + \Delta_2], & \tilde{d}_{A_2} &= -\frac{2 + \hat{\alpha}_s (2C_{A_1} + C_{A_2}(\omega - 1))}{\sqrt{3}} \Delta_1, & \tilde{d}_{A_3} &= \frac{1 - \omega}{\sqrt{3}} C_{A_3} \hat{\alpha}_s \Delta_1, \\
\tilde{d}_{T_1} &= -\frac{2m_{\Lambda_b}}{\sqrt{3} m_{\Lambda_{c,1/2}^*}} C_{T_3} \hat{\alpha}_s \Delta_1, & \tilde{d}_{T_2} &= -\frac{2 + \hat{\alpha}_s (2(C_{T_1} + C_{T_3}) + (\omega - 1)C_{T_2})}{\sqrt{3}} \Delta_1, \\
\tilde{d}_{T_3} &= \frac{m_{\Lambda_b} (1 + \omega)}{\sqrt{3} m_{\Lambda_{c,1/2}^*}} C_{T_3} \hat{\alpha}_s \Delta_1, & \tilde{d}_{T_4} &= \frac{(1 - \omega)(1 + \hat{\alpha}_s (C_{T_1} - C_{T_2} + C_{T_3})) \Delta_1 - \Delta_2}{\sqrt{3}}, \\
\tilde{l}_S &= (1 + C_S \hat{\alpha}_s) \Omega_1 + (\omega - 1) \Omega_2, & \tilde{l}_P &= (1 + C_P \hat{\alpha}_s) \Omega_1 + (\omega + 1) \Omega_2, \\
\tilde{l}_{V_1} &= (1 + C_{V_1} \hat{\alpha}_s) \Omega_1 + (\omega + 1) \Omega_2, & \tilde{l}_{V_2} &= C_{V_2} \hat{\alpha}_s \Omega_1 - 2\Omega_2, & \tilde{l}_{V_3} &= C_{V_3} \hat{\alpha}_s \Omega_1, \\
\tilde{l}_{A_1} &= (1 + C_{A_1} \hat{\alpha}_s) \Omega_1 + (\omega - 1) \Omega_2, & \tilde{l}_{A_2} &= C_{A_2} \hat{\alpha}_s \Omega_1 - 2\Omega_2, & \tilde{l}_{A_3} &= C_{A_3} \hat{\alpha}_s \Omega_1 \\
\tilde{l}_{T_2} &= 2\Omega_2 - C_{T_2} \hat{\alpha}_s \Omega_1, & \tilde{l}_{T_3} &= -\frac{m_{\Lambda_b}}{m_{\Lambda_{c,3/2}^*}} C_{T_3} \hat{\alpha}_s \Omega_1, & \tilde{l}_{T_4} &= (1 + C_{T_1} \hat{\alpha}_s) \Omega_1 + (\omega - 1) \Omega_2. \\
\end{aligned} \tag{B1}$$

TABLE I. Numerical values of  $\hat{\alpha}_s C_{\Gamma_i}(\omega = 1)$  used in this work as obtained from Ref. [42].

	$\hat{\alpha}_s C_S$	$\hat{\alpha}_s C_P$	$\hat{\alpha}_s C_{V_1}$	$\hat{\alpha}_s C_{V_2}$	$\hat{\alpha}_s C_{V_3}$	$\hat{\alpha}_s C_{A_1}$	$\hat{\alpha}_s C_{A_2}$	$\hat{\alpha}_s C_{A_3}$	$\hat{\alpha}_s C_{T_1}$	$\hat{\alpha}_s C_{T_2}$	$\hat{\alpha}_s C_{T_3}$
$\times 10^2$	-5.52	5.52	7.59	-3.85	-1.67	-3.44	-9.96	3.44	2.77	-7.69	3.34

The numerical inputs for the radiative corrections are  $\alpha(\sqrt{m_b m_c}) = 0.26$  and  $z = m_c/m_b = 1.38/4.78 \sim 0.29$  as in Ref. [7]. The form factors not listed above, i.e.,  $\tilde{l}_{V_4}, \tilde{l}_{A_4}, \tilde{l}_{T_1}, \tilde{l}_{T_3}, \tilde{l}_{T_6}$ , vanish at this order. The radiative

corrections produce small effects, of the order of few percent, in the HQET predictions. To illustrate this, we give in Table I the values of  $\hat{\alpha}_s C_{\Gamma_i}(\omega = 1)$  obtained from Appendix A of Ref. [42].

- 
- [1] A. K. Leibovich and I. W. Stewart, Semileptonic Lambda(b) decay to excited Lambda(c) baryons at order Lambda(QCD)/m(Q), *Phys. Rev. D* **57**, 5620 (1998).
- [2] M. Pervin, W. Roberts, and S. Capstick, Semileptonic decays of heavy lambda baryons in a quark model, *Phys. Rev. C* **72**, 035201 (2005).
- [3] T. Yoshida, E. Hiyama, A. Hosaka, M. Oka, and K. Sadato, Spectrum of heavy baryons in the quark model, *Phys. Rev. D* **92**, 114029 (2015).
- [4] H. Nagahiro, S. Yasui, A. Hosaka, M. Oka, and H. Noumi, Structure of charmed baryons studied by pionic decays, *Phys. Rev. D* **95**, 014023 (2017).
- [5] P. Böer, M. Bordone, E. Graverini, P. Owen, M. Rotondo, and D. Van Dyk, Testing lepton flavour universality in semileptonic  $\Lambda_b \rightarrow \Lambda_c^*$  decays, *J. High Energy Phys.* **06** (2018) 155.
- [6] S. Meinel and G. Rendon,  $\Lambda_b \rightarrow \Lambda_c^*(2595, 2625)\ell^-\bar{\nu}$  form factors from lattice QCD, *Phys. Rev. D* **103**, 094516 (2021).
- [7] M. Papucci and D. J. Robinson, Form factor counting and HQET matching for new physics in  $\Lambda_b \Lambda_c^* \ell \nu$ , *Phys. Rev. D* **105**, 016027 (2022).
- [8] S. Migura, D. Merten, B. Metsch, and H.-R. Petry, Charmed baryons in a relativistic quark model, *Eur. Phys. J. A* **28**, 41 (2006).
- [9] H. Garcilazo, J. Vijande, and A. Valcarce, Faddeev study of heavy baryon spectroscopy, *J. Phys. G* **34**, 961 (2007).
- [10] W. Roberts and M. Pervin, Heavy baryons in a quark model, *Int. J. Mod. Phys. A* **23**, 2817 (2008).
- [11] A. J. Arifi, H. Nagahiro, and A. Hosaka, Three-body decay of  $\Lambda_c^*(2595)$  and  $\Lambda_c^*(2625)$  with consideration of  $\Sigma_c(2455)\pi$  and  $\Sigma_c^*(2520)\pi$  in intermediate states, *Phys. Rev. D* **95**, 114018 (2017).
- [12] M. F. M. Lutz and E. E. Kolomeitsev, On charm baryon resonances and chiral symmetry, *Nucl. Phys. A* **730**, 110 (2004).
- [13] L. Tolos, J. Schaffner-Bielich, and A. Mishra, Properties of D-mesons in nuclear matter within a self-consistent coupled-channel approach, *Phys. Rev. C* **70**, 025203 (2004).
- [14] J. Hofmann and M. F. M. Lutz, Coupled-channel study of crypto-exotic baryons with charm, *Nucl. Phys. A* **763**, 90 (2005).
- [15] T. Mizutani and A. Ramos, D mesons in nuclear matter: A DN coupled-channel equations approach, *Phys. Rev. C* **74**, 065201 (2006).
- [16] J. Hofmann and M. F. M. Lutz, D-wave baryon resonances with charm from coupled-channel dynamics, *Nucl. Phys. A* **776**, 17 (2006).
- [17] C. Garcia-Recio, V. K. Magas, T. Mizutani, J. Nieves, A. Ramos, L. L. Salcedo, and L. Tolos, The s-wave charmed baryon resonances from a coupled-channel approach with heavy quark symmetry, *Phys. Rev. D* **79**, 054004 (2009).
- [18] O. Romanets, L. Tolos, C. Garcia-Recio, J. Nieves, L. L. Salcedo, and R. G. E. Timmermans, Charmed and strange baryon resonances with heavy-quark spin symmetry, *Phys. Rev. D* **85**, 114032 (2012).
- [19] J.-X. Lu, Y. Zhou, H.-X. Chen, J.-J. Xie, and L.-S. Geng, Dynamically generated  $J^P = 1/2^-(3/2^-)$  singly charmed and bottom heavy baryons, *Phys. Rev. D* **92**, 014036 (2015).
- [20] J.-X. Lu, H.-X. Chen, Z.-H. Guo, J. Nieves, J.-J. Xie, and L.-S. Geng,  $\Lambda_c(2595)$  resonance as a dynamically generated state: The compositeness condition and the large  $N_c$  evolution, *Phys. Rev. D* **93**, 114028 (2016).
- [21] J. A. Oller and U. G. Meissner, Chiral dynamics in the presence of bound states: Kaon nucleon interactions revisited, *Phys. Lett. B* **500**, 263 (2001).
- [22] C. Garcia-Recio, J. Nieves, E. Ruiz Arriola, and M. J. Vicente Vacas,  $S = -1$  meson baryon unitarized coupled channel chiral perturbation theory and the S(01) Lambda(1405) and Lambda(1670) resonances, *Phys. Rev. D* **67**, 076009 (2003).
- [23] C. Garcia-Recio, M. F. M. Lutz, and J. Nieves, Quark mass dependence of s wave baryon resonances, *Phys. Lett. B* **582**, 49 (2004).
- [24] T. Hyodo and D. Jido, The nature of the Lambda(1405) resonance in chiral dynamics, *Prog. Part. Nucl. Phys.* **67**, 55 (2012).
- [25] J. Nieves, R. Pavao, and S. Sakai,  $\Lambda_b$  decays into  $\Lambda_c^*\ell\bar{\nu}_\ell$  and  $\Lambda_c^*\pi^-$  [ $\Lambda_c^* = \Lambda_c(2595)$  and  $\Lambda_c(2625)$ ] and heavy quark spin symmetry, *Eur. Phys. J. C* **79**, 417 (2019).
- [26] W. H. Liang, T. Uchino, C. W. Xiao, and E. Oset, Baryon states with open charm in the extended local hidden gauge approach, *Eur. Phys. J. A* **51**, 16 (2015).

- [27] J. Nieves and R. Pavao, Nature of the lowest-lying odd parity charmed baryon  $\Lambda_c(2595)$  and  $\Lambda_c(2625)$  resonances, *Phys. Rev. D* **101**, 014018 (2020).
- [28] T. Mannel, W. Roberts, and Z. Ryzak, Baryons in the heavy quark effective theory, *Nucl. Phys.* **B355**, 38 (1991).
- [29] N. Isgur and M. B. Wise, Heavy baryon weak form-factors, *Nucl. Phys.* **B348**, 276 (1991).
- [30] W. Roberts, Semileptonic decays of heavy Lambda's into excited baryons, *Nucl. Phys.* **B389**, 549 (1993).
- [31] S. Meinel and G. Rendon,  $\Lambda_c\Lambda^*(1520)$  form factors from lattice QCD and improved analysis of the  $\Lambda_b\Lambda^*(1520)$  and  $\Lambda_b\Lambda_c^*(2595, 2625)$  form factors, *Phys. Rev. D* **105**, 054511 (2022).
- [32] T. Gutsche, M. A. Ivanov, J. G. Körner, V. E. Lyubovitskij, V. V. Lyubushkin, and P. Santorelli, Theoretical description of the decays  $\Lambda_b \rightarrow \Lambda^{(*)}(\frac{1}{2}^\pm, \frac{3}{2}^\pm) + J/\psi$ , *Phys. Rev. D* **96**, 013003 (2017).
- [33] D. Bečirević, A. Le Yaouanc, V. Morénas, and L. Oliver, Heavy baryon wave functions, Bakamjian-Thomas approach to form factors, and observables in  $\Lambda_b \rightarrow \Lambda_c(\frac{1}{2}^\pm)\ell\bar{\nu}$  transitions, *Phys. Rev. D* **102**, 094023 (2020).
- [34] K. C. Bowler, R. D. Kenway, L. Lellouch, J. Nieves, O. Oliveira, D. G. Richards, C. T. Sachrajda, N. Stella, and P. Ueberholz (UKQCD Collaboration), First lattice study of semileptonic decays of Lambda-b and Xi-b baryons, *Phys. Rev. D* **57**, 6948 (1998).
- [35] S. A. Gottlieb and S. Tamhankar, A lattice study of Lambda(b) semileptonic decay, *Nucl. Phys. B, Proc. Suppl.* **119**, 644 (2003).
- [36] W. Detmold, C. Lehner, and S. Meinel,  $\Lambda_b \rightarrow p\ell^-\bar{\nu}_\ell$  and  $\Lambda_b \rightarrow \Lambda_c\ell^-\bar{\nu}_\ell$  form factors from lattice QCD with relativistic heavy quarks, *Phys. Rev. D* **92**, 034503 (2015).
- [37] A. Datta, S. Kamali, S. Meinel, and A. Rashed, Phenomenology of  $\Lambda_b \rightarrow \Lambda_c\tau\bar{\nu}_\tau$  using lattice QCD calculations, *J. High Energy Phys.* **08** (2017) 131.
- [38] R. Aaij *et al.* (LHCb Collaboration), Measurement of the shape of the  $\Lambda_b^0 \rightarrow \Lambda_c^+\mu^-\bar{\nu}_\mu$  differential decay rate, *Phys. Rev. D* **96**, 112005 (2017).
- [39] M. A. Shifman, N. G. Uraltsev, and A. I. Vainshtein, V(cb) from OPE sum rules for heavy flavor transitions, *Phys. Rev. D* **51**, 2217 (1995); Erratum, *Phys. Rev. D* **52**, 3149 (1995).
- [40] I. I. Y. Bigi, M. A. Shifman, N. G. Uraltsev, and A. I. Vainshtein, Sum rules for heavy flavor transitions in the SV limit, *Phys. Rev. D* **52**, 196 (1995).
- [41] M.-L. Du, N. Penalva, E. Hernández, and J. Nieves, New physics effects on  $\Lambda_b \rightarrow \Lambda_c^*\tau\bar{\nu}_\tau$  decays, *Phys. Rev. D* **106**, 055039 (2022).
- [42] F. U. Bernlochner, Z. Ligeti, M. Papucci, and D. J. Robinson, Combined analysis of semileptonic  $B$  decays to  $D$  and  $D^*$ :  $R(D^{(*)})$ ,  $|V_{cb}|$ , and new physics, *Phys. Rev. D* **95**, 115008 (2017); Erratum, *Phys. Rev. D* **97**, 059902 (2018).
- [43] A. F. Falk, Hadrons of arbitrary spin in the heavy quark effective theory, *Nucl. Phys.* **B378**, 79 (1992).
- [44] M. Neubert, Heavy quark symmetry, *Phys. Rep.* **245**, 259 (1994).
- [45] Y. Aoki *et al.* (RBC, UKQCD Collaborations), Continuum limit physics from  $2+1$  flavor domain wall QCD, *Phys. Rev. D* **83**, 074508 (2011).
- [46] T. Blum *et al.* (RBC, UKQCD Collaborations), Domain wall QCD with physical quark masses, *Phys. Rev. D* **93**, 074505 (2016).
- [47] P. A. Zyla *et al.* (Particle Data Group), Review of particle physics, *Prog. Theor. Exp. Phys.* **2020**, 083C01 (2020).
- [48] T. Aaltonen *et al.* (CDF Collaboration), First measurement of the ratio of branching fractions  $B(\Lambda_b^0 \rightarrow \Lambda_c^+\mu^-\bar{\nu}_\mu)/B(\Lambda_b^0 \rightarrow \Lambda_c^+\pi^-)$ , *Phys. Rev. D* **79**, 032001 (2009).